

Scattering of compact oscillons

F. M. Hahne,^{1,*} P. Klimas,^{1,†} J. S. Streibel,¹ and W. J. Zakrzewski²

¹*Departamento de Física, Universidade Federal de Santa Catarina,
Campus Trindade, 88040-900, Florianópolis-SC, Brazil*

²*Department of Mathematical Sciences, Durham University, Durham DH1 3LE, U.K.*

We study various aspects of the scattering of generalized compact oscillons in the signum-Gordon model in (1+1) dimensions. Using covariance of the model we construct traveling oscillons and study their interactions and the dependence of these interactions on the oscillons' initial velocities and their relative phases. The scattering processes transform the two incoming oscillons into two outgoing ones and lead to the generation of extra oscillons which appear in the form of jet-like cascades. Such cascades vanish for some values of free parameters and the scattering processes, even though our model is non-integrable, resemble typical scattering processes normally observed for integrable or quase-integrable models.

Occasionally, in the intermediate stage of the process, we have seen the emission of shock waves and we have noticed that, in general, outgoing oscillons have been more involved in their emission than the initial ones *i.e.* they have a border in form of curved world-lines.

The results of our studies of the scattering of oscillons suggest that the radiation of the signum-Gordon model has a fractal-like nature.

PACS numbers:

I. INTRODUCTION

Oscillons are localized, time dependent, quasi-periodic solutions observed in many scalar field models. Their presence was first reported in [1]. In a vast majority of cases, in which physical models are non-integrable, oscillons radiate very slowly [2–13]. Oscillons can be created in some dynamical processes like, for instance, in kink-antikink collisions [9, 14–18]. On the other hand, oscillating structures seen in some integrable models, like (*e.g.* sine-Gordon model [19–21], affine Toda models [22] and non-linear Schrodinger model [23, 24]) do not radiate at all and so they can live forever. Such infinitely long living objects have special name “breathers” which distinguishes them from standard oscillons.

In this paper we describe our study of another interesting group of oscillons which share many properties of oscillons and breathers. A solution of such a type was first discovered in the signum-Gordon model [25]. The signum-Gordon oscillon is an exact solution which, if not perturbed, behaves like a breather *i.e.* it can live forever without emitting any radiation. This is a very interesting and extremely rare behaviour for time dependent solutions in non-integrable field theories. Of course, due to a non-integrable character of the model the perturbed signum-Gordon oscillon emits some radiation. Such radiation often takes the form of emissions of smaller oscillon-like

*CNPq Scholarship holder – Brazil

†Electronic address: pawel.klimas@ufsc.br

packages. So, this type of an oscillon can be thought of as being a stable (or perhaps metastable) time dependent and non-topological solution of a non-integrable model. Moreover, some very special perturbations of such oscillons lead to more general, exact and infinitely long lived oscillons (generalized oscillons). Such oscillons were constructed in [26, 27].

The signum-Gordon model [28] is perhaps the simplest example of a wider class of scalar field-theoretic models with non-analytic potentials. A very important and characteristic property of such models is their possession of compactons [29–34] and scaling symmetry [35]. This symmetry makes these models relevant in the description of dynamics of fields in other models with approximate scaling symmetry in the limit of small amplitudes [36–39]. In other words, the signum-Gordon model can be thought of as emerging, in this limit, from models containing non-analytic potentials. This demonstrates that studies of solutions of this model are useful and can have relevance in the description of some aspects of solutions of other models with non-analytic potentials. Of course, due to an often encountered rich structure of minima of such more general models, the field configurations with larger amplitudes could also have some nontrivial topology (kinks, skyrmions etc) [5, 29, 36, 40] and so their complete dynamics would be essentially different from the dynamics of the signum-Gordon compactons.

In what follows we present some basic notions about the signum-Gordon model. The model is defined by the Lagrangian density

$$\mathcal{L} = \frac{1}{2} \partial_\mu \phi \partial^\mu \phi - |\phi| \quad (\text{I.1})$$

and its dynamics is described by solutions of the Euler-Lagrange equation

$$\partial_\mu \partial^\mu \phi + \text{sgn}(\phi) = 0. \quad (\text{I.2})$$

The Euler-Lagrange equations contain a term $\frac{\partial}{\partial \phi} |\phi| = \pm 1$ and so they do not include the vacuum solution $\phi = 0$. In order to include explicitly the vacuum solution into a set of solutions of (I.2) we require that $\text{sgn}(0) := 0$. The model (I.1) has naturally appeared in the study of behaviour of scalar fields in the vicinity of minima of V-shaped potentials *i.e.* potentials whose left and right side derivatives at minima are different from each other. Such models are perfectly well-defined from a physical point of view. Moreover, in some cases they can be seen as field-theoretic limits of certain mechanical models, which certainly admit experimental realizations. In fact, it was such mechanical models that led to scalar field models with non-analytic potentials [29].

The physical origin of models with non-analytic potentials is wider than the continuous limit of mechanical models. Quite recently it has been reported in [36] that models with V-shaped potentials may be obtained from other physical models when a parametrization associated with a symmetry reduction leads to new field variables that are restricted, *i.e.* they cannot take arbitrarily high (or small) values. In the case of models with mechanical realisation such a restriction is *a priori* imposed on the system. The restrictions on values of fields lead to certain inconvenience in the description of dynamics of the system which, in such a case, is governed by both the Euler-Lagrange equations and the extra condition on the time derivative of the field. For instance, the mechanical model, in which the signum-Gordon model originates, has a continuous limit described by the field variable that satisfies $\tilde{\phi} \geq 0$. Thus the model possesses the potential with an infinite

barrier at $\tilde{\phi} = 0$ *i.e.* $\tilde{V}(\tilde{\phi}) = \tilde{\phi}$ for $\tilde{\phi} \geq 0$ and $\tilde{V}(\tilde{\phi}) = \infty$ for $\tilde{\phi} < 0$. The field must also satisfy the reflection condition $\partial_t \tilde{\phi} \rightarrow -\partial_t \tilde{\phi}$ at $\tilde{\phi} = 0$. One can avoid such an inconvenient reflection condition by considering an auxiliary model with a new field $\phi \in (-\infty, \infty)$ and the potential $V(\phi) = |\phi|$.¹ This new model is so-called *unfolded model*. The dynamics of the auxiliary field is mapped onto a dynamics of the physical field through the *folding transformation*, see [28]. Thus the signum-Gordon model and other models of this type can describe behaviour of physical systems with restrictions on values of scalar fields.

The signum-Gordon model is certainly non-integrable. This conclusion can be drawn from the existence of radiation in numerical simulations of generic initial field configurations. In fact, very little is known about the nature of this radiation. In this paper we describe results of our study of some aspects of radiation in the signum-Gordon model. We pay particular attention to the exact time-dependent solutions of the model known as compact oscillons² [25, 26], which are our principal candidates for constituents of the radiation. The signum-Gordon oscillons rely on three principal properties of models with V -shaped potentials: existence of compact solutions, scale invariance (exact or approximate) and lack of linearization of small amplitude oscillations. The existence of compact solutions, like compact oscillons in particular, follows from the fact that models with standard kinetic and gradient terms in the Lagrangian approach vacuum in a quadratic manner if the potential has a V -shaped form at the minimum [29]. The scale invariance [35] is a straightforward consequence of the form of the field equations. In the case of the signum-Gordon model the scale invariance is exact because $\text{sgn}(\phi)$ is a scale invariant term. A very important consequence of this fact is the existence the self-similar solutions and oscillons in all scales of energy and length. Thus the perturbed oscillons may lose energy by the emission of smaller (perturbed) oscillons. We shall demonstrate in this paper that this is really the case and that the oscillons are main ingredients of the radiation of the signum-Gordon model. Finally, the absence of linear small amplitude oscillations follows from the fact that $\text{sgn}(\phi)$ term cannot be linearized at $\phi = 0$. This implies that, independently of their size, the signum-Gordon oscillons are fundamentally non-linear field configurations.

The existence of many exact solutions of the signum-Gordon model in (1+1) dimensions follows from the fact that equation (I.2) reduces to a non-homogeneous wave equation on the segments of the x axis, where the sign of the scalar field is fixed, and so it has the general solution

$$\phi(t, x) = F(x + t) + G(x - t) + \frac{1}{4}(x^2 - t^2), \quad (\text{I.3})$$

where F and G are arbitrary functions. The main point here is that this reduction is local *i.e.* the size and localization of the segments of constant sign changes with time. This is a direct manifestation of a non-linear character of the model. Solutions like (I.3) are called *partial solutions*. The exact global solution of the model is given by an explicitly known set of properly patched partial solutions and it must hold for arbitrary times. Determining such a closed set of partial solutions

¹ This potential implies the term $\text{sgn}(\phi) = \frac{dV}{d\phi}$ in the field equations what justifies the name of the model.

² In the literature the infinitely long lived oscillons are more often called breathers than oscillons. Here we keep the name oscillon following the original paper [25].

is usually associated with certain technical difficulties. They correspond to an unpleasant side of finding solutions of models with V -shaped potentails.

The main aim of this paper is to describe the results of our study of interaction between two oscillons. Our motivation for such a study follows from the fact that in numerical simulations of models with V -shaped potentials [38] we have indeed observed collisions of oscillon-like structures in emerging radiation. The study of systems containing colliding oscillons may shade new light on the nature of the radiation of the signum-Gordon model. In particular we are interested in scattering processes involving just two oscillons. Unfortunately, even such a ‘simple’ scattering process is too complicated for a purely analytical investigation. For this reason we have used the numerical analysis as our principal tool and have restricted our attention to initial field configurations with certain symmetries. Our results can find applications not only for models with a single minimum potential but also for other models with multi V -shaped minima that can support the existence of compact kinks etc.

The paper is organized as follows. In Section II we present some facts about generalized oscillons with vanishing total linear momentum. Then making use of the Lorentz covariance of the model we construct traveling oscillons. In Section III we study scattering of two oscillons. Due to the compactness of the oscillons we take initial configurations by a simple superposition of non-overlapping oscillons. Further on in this section we also discuss shock waves and oscillons with non uniformly moving borders. The last section contains summary of our results and some comments.

II. GENERALIZED OSCILLON

A. Oscillons at rest

The generalized oscillon [26] is a periodic solution of the signum-Gordon model, parametrized by the continuous parameter v . Its borders move periodically from left to right and vice versa. The standard oscillon [25] is a particular case of the generalized one – for $v = 0$.

Here we consider generalized oscillons because our aim is to study oscillons which appear in the radiation of the signum-Gordon type models. Of course there is no reason to expect that only the solution with $v = 0$ would be present in the radiation. Recently has been discovered a wider class of oscillons in the signum-Gordon model [27] which is further generalization of uniformly swaying oscillons reported in [26]. Such generic oscillons can be present in the radiation spectrum of the signum-Gordon model. Due to their complexity we shall present such oscillons in a further part of the paper. Below we shall describe a simpler class of generalized oscillons [26] adopting new notation.

In our work here we are particularly interested in generalized oscillons which are in uniform motion (modulo a periodic motion given by v) in a certain reference frame S . We shall refer to this frame as to *the laboratory reference frame*. Moreover, we preserve symbols t and x for coordinates exclusively in this reference frame. On the other hand, the reference frame of the oscillon is denoted by S' and called *rest frame of the oscillon*. The precise meaning of expression “rest frame” in the case of swaying oscillons is the following one: it is the inertial reference frame in which the total

linear momentum of the oscillon vanishes. Space time coordinates in S' are denoted by t' and x' .

The basic oscillon has period $T = 1$. Smaller and bigger oscillons, which differ by their period, can be obtained from the basic one by the scaling transformation which exploits the scaling symmetry of the signum-Gordon equation. The Minkowski diagram presented in Fig.1 shows regions of validity of the partial solutions $\phi_k(t', x')$, $k = \{C, L_1, L_2, L_3, R_1, R_2, R_3\}$ that the oscillon consists on. These partial solutions are given by quadratic polynomials in variables t' and x' in rest frame of the oscillon. A physical part of polynomial solutions is restricted to some intervals of t' and x' . In order to get a periodic solution for any t' one has to replace t' by a periodic function of t' . Below we discuss this process in detail.

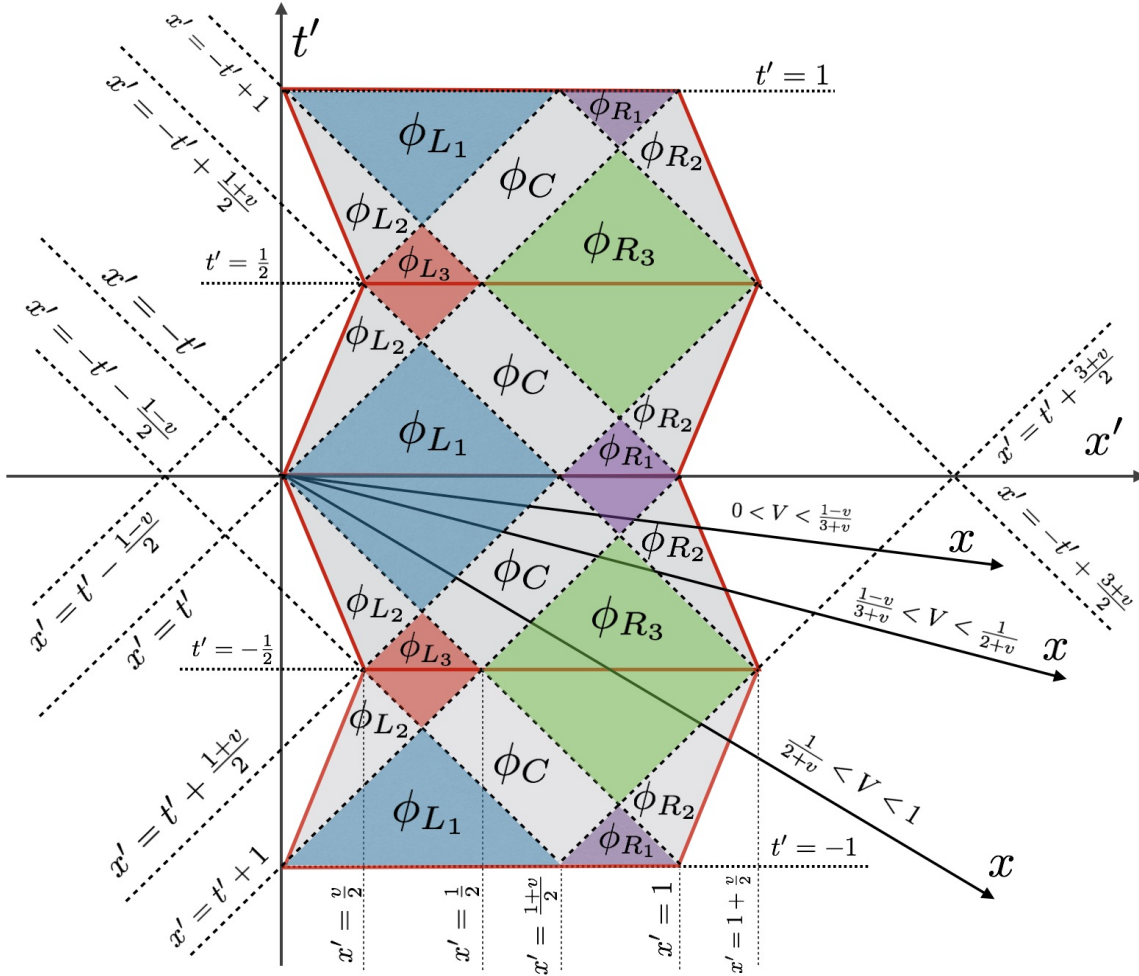


FIG. 1: The world sheet of the generalized oscillon seen in its own rest frame S' . Only in the interval $t' \in [0, \frac{1}{2}]$ it holds $\phi_k = \varphi_k$; other partial solutions are given by (II.9). The axes x of the laboratory reference frame seen in frame S' have an inclination with respect to axis x' . Here we present three different cases of inclination corresponding to the velocity $u' = -V$ of the laboratory frame S that moves to the left on the diagram S' . The angle of this inclination between axes x' and x is given by $\arctan(V)$.

We start our discussion with a set of partial solutions which are valid *only* in the interval $t' \in [0, \frac{1}{2}]$. These solutions have been given in [26] and they are denoted by the letter φ . Here, we

present them in a new notation. In fact, there are seven partial solutions in the interval $t' \in [0, \frac{1}{2}]$. Among them, four solutions are essentially different, namely

$$\varphi_C(t', x'; v) = \frac{(1+v-2x')^2 - 4t'(1+v-2vx') + 4(2-v^2)t'^2}{8(1-v^2)}, \quad (\text{II.1})$$

$$\varphi_{L_1}(t', x'; v) = \frac{t'^2}{2} - \frac{t'x'}{1+v}, \quad (\text{II.2})$$

$$\varphi_{L_2}(t', x'; v) = -\frac{(x' - vt')^2}{2(1-v^2)}, \quad (\text{II.3})$$

$$\varphi_{L_3}(t', x'; v) = \frac{1}{2} \left(t' - \frac{1}{2} \right) \left(t' + \frac{1}{2} + \frac{2x' - 1}{1-v} \right). \quad (\text{II.4})$$

The other three partial solutions $\varphi_{R_j}(t', x'; v)$, $j = 1, 2, 3$ can be obtained from those shown above by performing the transformation

$$x' \rightarrow 1 - x', \quad v \rightarrow -v \quad (\text{II.5})$$

which gives

$$\varphi_{R_j}(t', x'; v) = \varphi_{L_j}(t', 1 - x'; -v). \quad (\text{II.6})$$

Note that the solution $\varphi_C(t, x; v)$ is invariant under this transformation. Note also that all solutions $\varphi_k(t', x'; v)$ are negative-valued in their domains.

Each solution $\varphi_k(t', x'; v)$ is valid only in a specific region of the Minkowski diagram. For this reason we define a few region step functions $\Pi_k(t', x'; v)$ which are equal to unity only in the region in which a given partial solution holds and vanish outside this region:

$$\begin{aligned} \Pi_C(t', x'; v) &= \theta(x' - t')\theta(-x' - t' + 1)\theta(x' + t' - \frac{1+v}{2})\theta(-x' + t' + \frac{1+v}{2}), \\ \Pi_{L_1}(t', x'; v) &= \theta(x' - t')\theta(-x' - t' + \frac{1+v}{2}), \\ \Pi_{L_2}(t', x'; v) &= \theta(-x' + t')\theta(-x' - t' + \frac{1+v}{2})\theta(x' - vt'), \\ \Pi_{L_3}(t', x'; v) &= \theta(x' + t' - \frac{1+v}{2})\theta(-x' + t'), \\ \Pi_{R_j}(t', x'; v) &= \Pi_{L_j}(t', 1 - x', -v), \quad j = 1, 2, 3 \end{aligned}$$

where $\theta(z)$ is the unit step function $\theta(z) = 0$ for $z < 0$ and $\theta(z) = 1$ for $z \geq 0$. One can check that $\Pi_C(t', x'; v) = \Pi_C(t', 1 - x'; -v)$.

The parabolic functions like (II.1)-(II.4) are not periodic whereas the oscillon is a periodic solution. In order to give formulas which are valid for any t' , we define two periodic functions

$$\tau(z) := \frac{1}{\pi} \arcsin(|\sin(\pi z)|), \quad (\text{II.7})$$

$$\sigma(z) := \text{sgn}(\sin(2\pi z)), \quad (\text{II.8})$$

where $\tau(z)$ maps any t' onto the interval $[0, \frac{1}{2}]$ and $\sigma(z) = \pm 1$ agrees with classical derivative of $\tau(z)$. The functions (II.7) and (II.8) taken for $z \rightarrow t'$ allows to construct periodic solutions. The functions τ and σ are presented in Fig.2. The function $\sigma(z)$ is needed to describe the changes of

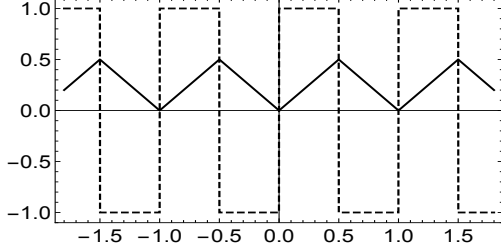


FIG. 2: Function $\tau(z)$ (solid line) and $\sigma(z)$ (dashed line).

the sign of partial solutions at $t' = \frac{n}{2}$. Any partial solution (for arbitrary t') can be written in terms of basic solutions $\varphi_k(t', x'; v)$, where $k = \{C, L_1, \dots, R_3\}$ that are valid only on the interval $t' \in [0, \frac{1}{2}]$. The partial solutions presented on the Minkowski diagram in Fig.1 have the form

$$\phi_k(t', x'; v) = \sigma(t') \varphi_k(\tau(t'), x'; v) \Pi_k(\tau(t'), x'; v). \quad (\text{II.9})$$

The functions (II.7) and (II.8) allow for more compact notation than that presented in [38]. Here the functions ϕ_{L_1/R_1}^- and ϕ_{L_3/R_3}^+ were be absorbed in definition of functions ϕ_{L_1/R_1} . Similarly, ϕ_{L_3/R_3}^- and ϕ_{L_1/R_1}^+ were be absorbed in definition of functions ϕ_{L_3/R_3} . The total solution is given by a continuous function which is a sum of non overlapping partial solutions (II.9). The derivative of the oscillon solution with respect to time is given by

$$\partial_{t'} \phi_k(t', x'; v) = \partial_z \varphi_k(z, x'; v)|_{z=\tau(t')} \Pi_k(\tau(t'), x'; v). \quad (\text{II.10})$$

where $\sigma^2(z) = 1$. Note that all the derivatives of the region step functions Π_α can be ignored because the sum of partial solutions is a continuous function so there is no reason to expect delta functions at the matching points.

In Fig.3 we present three snapshots of the oscillon solution $\phi(t', x'; v)$ and its time derivative $\partial_{t'} \phi(t', x'; v)$ at $t' = 0.1$, $t' = 0.4$ and $t' = 0.75$. Solutions presented in figures (a) and (d) consists on (from left to right) $\{\phi_{L_2}, \phi_{L_1}, \phi_C, \phi_{R_1}, \phi_{R_2}\}$, in figures (b) and (e) on $\{\phi_{L_2}, \phi_{L_3}, \phi_C, \phi_{R_3}, \phi_{R_2}\}$ and in figures (c) and (f) on $\{\phi_{L_2}, \phi_{L_1}, \phi_C, \phi_{R_3}, \phi_{R_2}\}$.

B. Travelling oscillons

The signum-Gordon equation

$$(\partial_t^2 - \partial_x^2) \phi(t, x) + \text{sgn } \phi(t, x) = 0 \quad (\text{II.11})$$

is invariant under the Lorentz transformations. Thus traveling compact oscillons can be obtained from the non traveling ones by an appropriate Lorentz transformation. In particular, the oscillon with non vanishing linear momentum is obtained from the generalized (with zero total linear momentum) oscillon by a Lorentz boost. In what follows we assume that the laboratory reference frame S moves with velocity $u' = \mp V$ with respect to the rest frame of the oscillon S' . Thus the

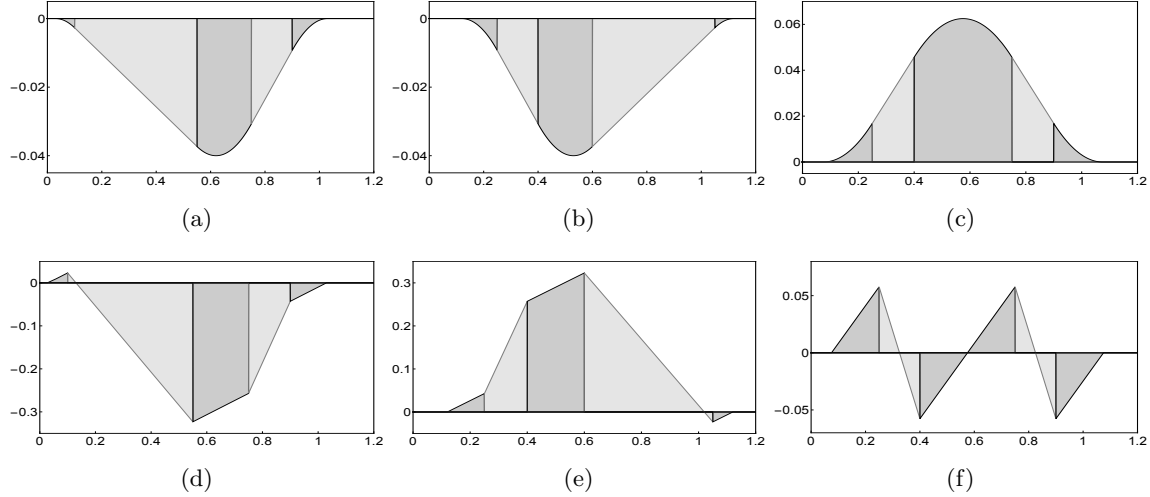


FIG. 3: The profile function $\phi(t', x'; v)$ of the generalized oscillon for $v = 0.3$ at (a) $t' = 0.1$, (b) $t' = 0.4$ and (c) $t' = 0.75$. The corresponding time derivatives of $\partial_{t'}\phi(t', x'; v)$ are shown in (d) at $t' = 0.1$, in (e) at $t' = 0.4$ and in (f) at $t' = 0.75$.

oscillon has velocity $u = \pm V$ in the laboratory frame S . The field configuration that corresponds with the traveling oscillon is a function of coordinates t and x and it is given by plugging

$$t' \rightarrow \xi := \frac{t - ux}{\sqrt{1 - u^2}}, \quad x' \rightarrow \zeta := \frac{x - ut}{\sqrt{1 - u^2}} \quad (\text{II.12})$$

into (II.9) giving partial solutions

$$\psi_k(t, x; v, u) := \sigma(\xi)\varphi_k\left(\tau(\xi), \zeta; v\right)\Pi_k\left(\tau(\xi), \zeta; v\right), \quad (\text{II.13})$$

The derivative of the field with respect to time t is given by expression

$$\partial_t\psi_k(t, x; v, u) = \frac{1}{\sqrt{1 - u^2}} \left[\partial_{\bar{\xi}}\varphi_k(\bar{\xi}, \bar{\zeta}; v) - u\sigma(\xi)\partial_{\bar{\zeta}}\varphi_k(\bar{\xi}, \bar{\zeta}; v) \right] \Pi_k(\bar{\xi}, \bar{\zeta}; v) \Big|_{\bar{\xi}=\tau(\xi), \bar{\zeta}=\zeta}, \quad (\text{II.14})$$

where $\frac{d}{dz}\tau(z) = \sigma(z)$ and $\sigma^2(z) = 1$ at open supports of partial solutions. Hence, the travelling oscillon in S is a solution of (II.11) given by a sum of non overlapping partial solutions (II.13), namely

$$\psi(t, x; v, u) = \sum_k \psi_k(t, x; v, u), \quad (\text{II.15})$$

where $k = \{L_1, L_2, L_3, C, R_1, R_2, R_3\}$.

Note, that the axis x' *i.e* the line $t' = 0$ in S' is not a simultaneity line in S . The scalar field $\phi(t', x'; v)$ vanishes at horizontal lines $t' = \frac{n}{2}$, $n = 0, \pm 1, \pm 2, \dots$ which are shown in Fig.1. It means that the oscillon seen in the laboratory reference frame S has some isolated traveling zeros. Such isolated zeros are given by points of intersection of lines parallel to the axis x (given by $t = \text{const}$) with the lines $t' = \frac{n}{2}$. The number of isolated zeros and the composition of the oscillon (types of partial solutions seen in S at given instant of time t) depends on the value of the velocity $u = \pm V$

which the oscillon have in S . The axes x and x' form an angle $\arctan(V)$ so for $V < \frac{1}{2+v}$ there is only one point of intersection of straight lines parallel to x' with the line $t' = \frac{n}{2}$. For $\frac{1}{2+v} < V < 1$, a second isolated zero arises at some value of the time interval.

According to the diagram presented in Fig.1, the initial (at $t = 0$) configuration of the field in S , obtained by the Lorentz boost of the oscillon given in S' , consists of different sets of partial solutions corresponding to different values of the velocity V . Let us consider the oscillon that moves with the velocity $u = +V$ in the laboratory reference frame. The oscillon configuration ψ at $t = 0$ consists of (from left to right)

$$\{\psi_{L_1}, \psi_C, \psi_{R_1}, \psi_{R_2}\} \quad \text{for} \quad 0 < V < \frac{1-v}{3+v}, \quad (\text{II.16})$$

$$\{\psi_{L_1}, \psi_C, \psi_{R_3}, \psi_{R_2}\} \quad \text{for} \quad \frac{1-v}{3+v} < V < \frac{1}{2+v}, \quad (\text{II.17})$$

$$\{\psi_{L_1}, \psi_C, \psi_{R_3}, \psi_{R_2}\} \quad \text{for} \quad \frac{1}{2+v} < V < 1. \quad (\text{II.18})$$

The cases (II.17) and (II.18) differ by a sign of partial solutions ψ_{R_3} and ψ_{R_2} .

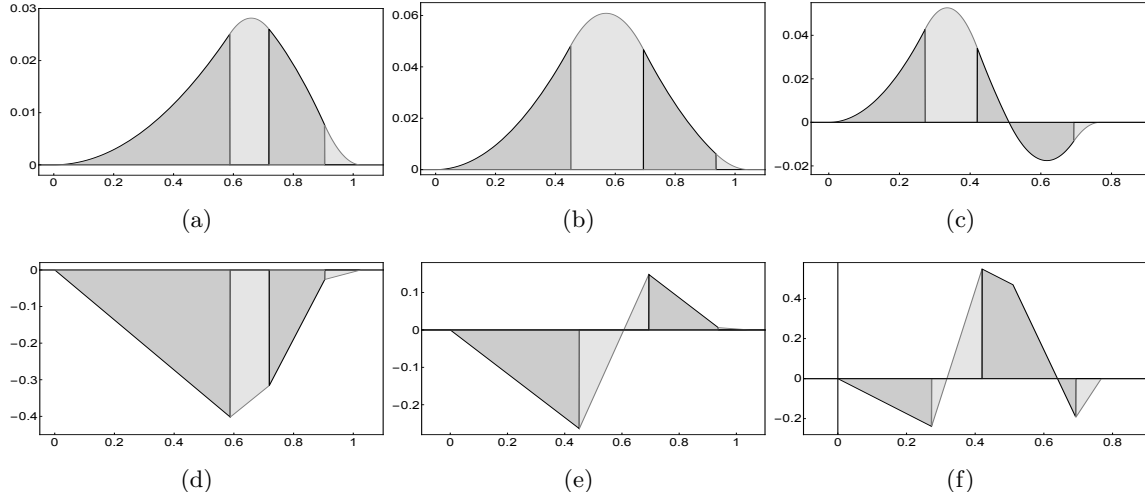


FIG. 4: The generalized oscillon with the velocity $u = +V$ in the laboratory reference frame at $t = 0$. The oscillon is parametrized by $v = 0.3$. Figures (a), (b), (c) show the initial shape of the oscillon $\psi(t, x; vV)|_{t=0}$ whereas (d), (e), (f) show $\partial_t\psi(t, x; v, V)|_{t=0}$. Figures (a), (d) correspond with the oscillon velocity $V = 0.1$, (b), (e) with $V = 0.35$ and (c), (f) with $V = 0.7$.

Fig.4 shows three examples of such field configurations and their time derivatives at $t = 0$. All three oscillons have $v = 0.3$ (it gives $\frac{1-v}{3+v} \approx 0.212$ and $\frac{1}{2+v} \approx 0.434$) and they differ by the value of velocity V . Figures (a) and (d) were obtained for $V = 0.1$ and they correspond with (II.16), (b) and (e) were obtained for $V = 0.35$ and they correspond with (II.17) and figures (c) and (f) show the case (II.18) with $V = 0.7$.

III. SCATTERING OF OSCILLONS

A. Initial configurations for scattering process

1. Two-oscillon configurations

Compactness of exact oscillons allows to construct some multi-oscillon configurations which are exact solutions of the signum-Gordon equation. The only condition is the non-overlapping the supports of individual oscillons. A generic initial configuration $\{\Psi(x), \Psi_t(x)\}$ containing two travelling oscillons is given by superposition of non-overlapping travelling oscillons obtained from generalized oscillons $\phi(t, x; v_1)$ and $\phi(t, x; v_2)$ by transformations which are symmetries of the signum-Gordon equation, namely

- Poincaré transformations in 1+1 dimensions: boosts, spatial and temporal translations, spatial and temporal reflections,
- symmetry of the scale $\phi(t, x) \rightarrow \phi^{(\lambda)}(t, x) = \lambda^2 \phi(\frac{t}{\lambda}, \frac{x}{\lambda})$,
- sign flipping of the field $\phi \rightarrow -\phi$.

Two individual oscillons, $i = 1, 2$, are obtained by transformations

$$\phi(t, x; v_i) \rightarrow \Psi_i(t, x) := \varepsilon_i \psi^{(\lambda_i)}(t + t_{0i}, \epsilon_i x + x_{0i}; v_i, u_i)$$

where u_i are boost velocities, t_{0i} are temporal translations, x_{0i} are spatial translations, λ_i stand for scale parameters and $\varepsilon_i = \pm 1$ and $\epsilon_i = \pm 1$ for reflections. We shall fix the sign of $v_i > 0$ because $\phi(t, x; -v) = \phi(t, 1 - x, v)$ which means that the sign of v can be absorbed in a combination of spatial reflexion and translation.

The initial configuration $\{\Psi(x), \Psi_t(x)\}$ is given by

$$\Psi(x) := \Psi_1(0, x) + \Psi_2(0, x), \quad (\text{III.1})$$

$$\Psi_t(x) := \partial_t \Psi_1(t, x)|_{t=0} + \partial_t \Psi_2(t, x)|_{t=0} \quad (\text{III.2})$$

where non-overlapping of their supports restrict values of admissible spatial translations.

It turns out that some of these parameters can be omitted without loss of generality. The only relevant initial configurations involving two oscillons are those which are not equivalent *i.e.* they can not be related by a single symmetry transformation. The set of relevant free parameters contain relative scale, relative velocity etc. In some cases it will be more convenient fix one of them and let the one be free.

In Fig.5 we present an example of initial configuration containing two oscillons which move in opposite directions with velocities $u_1 = 0.5$ and $u_2 = -0.7$. The configuration was obtained taking generalized oscillons with $v_1 = 0.3$ and $v_2 = 0.34$ and $\lambda_1 = \lambda_2 = 1$. We have set $t_0 = 0$ and $\varepsilon_i = 1$ as well as $\epsilon_i = 1$. The oscillons were shifted in space taking $x_{01} = 0$ and $x_{02} = -1.3$.

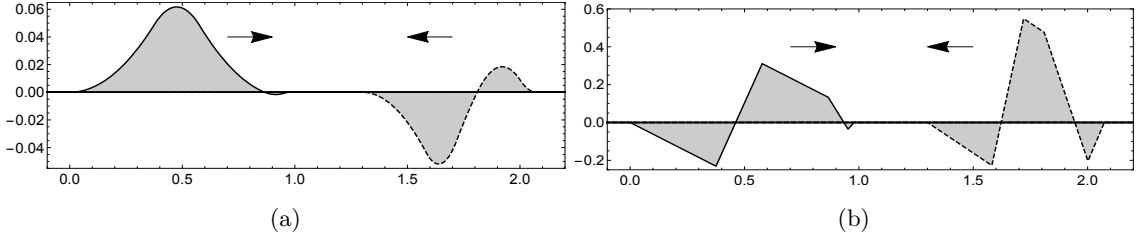


FIG. 5: Initial field configuration (a) $\Psi(x)$ and (b) $\Psi_t(x)$ given by two compact oscillons at $t = 0$. Parameters of oscillons $v_1 = 0.3$, $v_2 = 0.34$, $u_1 = 0.5$, $u_2 = -0.7$, $x_{01} = 0$, $x_{02} = -1.3$ and $t_{01} = t_{02} = 0$, $\lambda_i = 1$, $\varepsilon_i = 1 = \epsilon_i$ where $i = 1, 2$.

2. Symmetric configurations

A numerical study of the scattering process shows the process depends on many parameters like v_1 , v_2 , the relative velocity of the oscillons, their initial distance, time shift and reflections. In order to simplify the set of parameters we decided to restrict our considerations to *symmetric* and *anti-symmetric* initial configurations which certainly reduces the number of free parameters. It turned out that even with this restrictions we were left with sufficiently rich physical systems. We think that more general configurations are even interesting, however, their systematic study requires much more work so we decided put main effort on symmetric configurations.

In order to get a symmetric $\Psi^{(s)}$ and antisymmetric $\Psi^{(a)}$ configuration one can take a single oscillon parametrized by v and perform a sequence of symmetry transformations which leads to $\psi(t + t_0, x + x_0; v, u)|_{t=0}$, where the boost velocity is chosen $u = +V$ with $V \geq 0$. The second oscillon can be obtained from this result by spatial reflection $x \rightarrow -x$ and, optionally, by sign flipping. Naturally, x_0 must be chosen in the way that the support of ψ lies on negative semiaxis x . In such a case the support of the oscillon and its mirror image do not overlap. The initial symmetric and antisymmetric configurations are given by

$$\begin{aligned} \Psi^{(s/a)}(x) &= \psi(t + t_0, x + x_0; v, V)|_{t=0} \pm \psi(t + t_0, -x + x_0; v, V)|_{t=0} \\ \Psi_t^{(s/a)}(x) &= \partial_t \psi(t + t_0, x + x_0; v, V)|_{t=0} \pm \partial_t \psi(t + t_0, -x + x_0; v, V)|_{t=0} \end{aligned} \quad (\text{III.3})$$

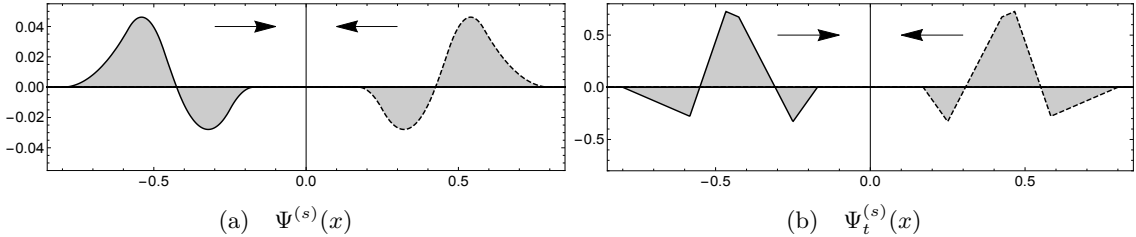


FIG. 6: Symmetric initial configuration of two compact oscillons parametrized by $V = 0.8$, $v = 0.3$, $t_0 = 0$ and $x_0 = 0.8$.

Fig. 6 shows a symmetric initial configuration $\{\Psi^{(s)}(x), \Psi_t^{(s)}(x)\}$ involving two compact oscillons. An antisymmetric configuration is obtained by flipping the sign of one oscillon.

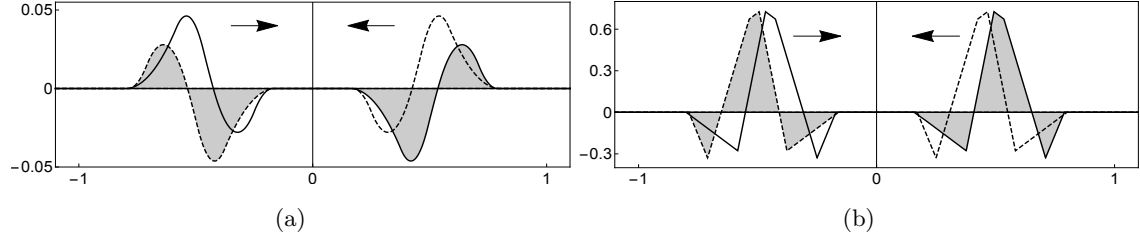


FIG. 7: Another possible symmetric initial configuration of two compact oscillons parametrized by $V = 0.8$, $v = 0.3$, $t_0 = 0$ and $x_0 = -0.16$.

Note that an alternative symmetric (antisymmetric) initial configuration can be obtained taking $u = -V$ and shifting the resulting oscillon to the right i.e. choosing $x_0 < 0$. The second oscillon is obtained by mirror reflection $x \rightarrow -x$ (and possibly the sign flip). An example of such initial configuration is shown in Fig.7 (shadowed regions). The configuration shown in Fig.6 is marked in Fig.7 by curves without shadowing.

3. Phase of the oscillon

Unlike for the case of compact kinks, the scattering process of two oscillons depends on the initial distance between them. This observation follows from the fact that the shape of the oscillons changes with time and the result of scattering process strongly depends³ on the shapes of oscillons at the moment when their supports begin to collide. Thus the *phase* of the oscillon is another relevant parameter which must be taken into account in the analysis of scattering of oscillons. Two traveling oscillons that differ *exclusively* by the value of spatial translation are said to have *the same phase*. The phase of the oscillon in its own rest frame S' is a number $\alpha \in [0, 1)$ where the lower limit $\alpha = 0$ represents oscillon configuration at $t' = 0$ and the upper limit $\alpha = 1 = T_{\text{rest}}$ (for $\lambda = 1$) corresponds with the period of the oscillon. The period of the oscillon in the laboratory reference frame S , in which the oscillon has certain velocity V , is given by $T_{\text{lab}} = \gamma \equiv (1 - V^2)^{-1/2}$ and the distance travelled during the period T_{lab} is γV , thus $\psi(t + \gamma, x + \gamma V; v, V) = \psi(t, x; v, V)$. The phase of the oscillon in the laboratory reference frame S can be chosen again as the number $\alpha \in [0, 1)$, where the upper limit is given by T_{lab}/γ . Note, that two oscillons with the same phase in two different inertial reference frames correspond with different field configurations. Below we describe in more detail the choice of the initial symmetric (antisymmetric) configuration containing two oscillons.

The uniform motion of the oscillons from $t = 0$ to the moment of collision results in a variation of their phases or variation of their common phase in the case of symmetric (antisymmetric) initial configuration. The variation of the phase depends on the initial distance between support of two oscillons. Since the oscillons do not interact until they supports begin to overlap one can eliminate this initial distance without loss of generality. This can be done choosing properly the value of

³ This observation follows from our numerical investigation and it will be discussed in further part of the paper.

spatial translation. The condition that oscillons begin to collide at $t = 0$ (their supports touch to each other) makes the parameter of spatial shift a function of the phase *i.e.* $x_0 = x_0(\alpha)$.

In order to set up the phase of oscillation at $t = 0$ one can make use of translational symmetry $t \rightarrow t + t_0$ of the signum-Gordon equation. Due to periodicity of the solution the parameter t_0 can be chosen as $t_0 = \alpha\gamma$. A sequence of oscillons with different phases α is plotted in Fig.8(a). Configurations $\alpha = 0$ and $\alpha = 1$ differ exclusively by spatial translation which means that they have equal phases. In Fig.8(b) we plot a worldsheet of the generalized oscillon in the laboratory

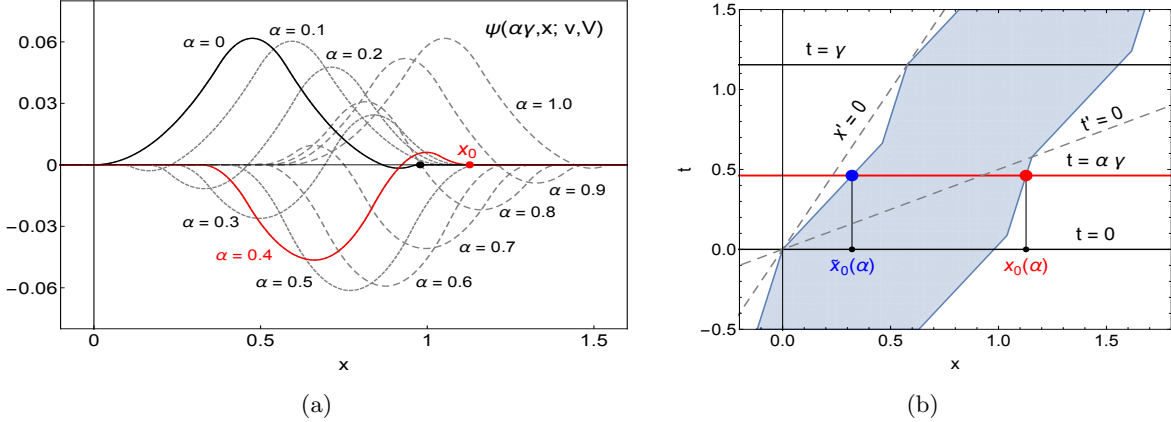


FIG. 8: (a) Oscillon $\psi(\gamma\alpha, x; v, V)$ with $V = 0.5$ and $v = 0.3$ for several values of α . (b) A worldsheet of the oscillon and the surface of simultaneity at $t = 0.4\gamma$ in the laboratory reference frame. The corresponding configuration is distinguished in figure (a).

reference frame where it moves with velocity $u = +V$. The endpoints of the oscillon are marked by $\tilde{x}(\alpha)$ (the left one) and $x(\alpha)$ (the right one). It is pretty clear from this diagram that the length of the oscillon in the laboratory reference frame

$$L(\alpha) = x(\alpha) - \tilde{x}(\alpha) \quad (\text{III.4})$$

is a periodic function of the time when $v \neq 0$ and it is equal to $1/\gamma$ (for $\lambda = 1$) when $v = 0$.

In order to get an initial configuration for the scattering process we translate the oscillon to the left by a distance $x_0(\alpha)$. The second oscillon is obtained by a mirror reflection of the first one. Hence the initial configurations that are subject of considerations in this paper are those given by (III.3) with $t_0 = \alpha\gamma$ and $x_0 = x_0(\alpha)$. In Fig.9 we plot initial profile of the field $\Psi^{(s)}(x)$ with different phases.

4. Determination of endpoints $x(\alpha)$ and $\tilde{x}(\alpha)$ of the oscillon

We start with determination of the function $x_0(\alpha)$ which describes position of *right endpoint* of the oscillon. It is enough to restrict considerations to $v \geq 0$ because any non-travelling oscillon satisfies relation $\phi(t, x; -v) = \phi(t, 1 - x)$. We shall consider here boosts in two directions, namely $u = \pm V$, where $0 \leq V < 1$. In all formulas containing “ \pm ” the upper sign corresponds with $u = +V$ and the lower one with $u = -V$.

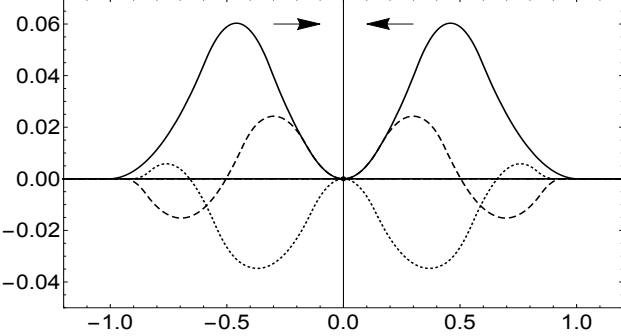


FIG. 9: Symmetric initial configurations of the oscillons $\Psi^{(s)}(x)$ at $t = 0$ when their supports begin to collide. The configurations correspond with $v = 0.2$, $V = \frac{1}{2+v} - 0.1 \approx 0.3545$. The phases of oscillations are given by $\alpha = 0$ (solid line), $\alpha = 0.1772$ (dashed line) and $\alpha = 0.6222$ (dotted line).

The simultaneity line $t = \alpha\gamma$ in the laboratory reference frame S has equation

$$t' = \alpha \mp Vx' \quad (\text{III.5})$$

in the reference frame of the oscillon S' . In coordinates in S' the right border of the oscillon is a worldline given by

$$x' = 1 + v\tau(t'), \quad (\text{III.6})$$

where $\tau(t')$ is a function defined in (II.7). Eliminating x' from (III.5) and (III.6) we find that $t'(\alpha)$ is a solution of the equation

$$\tau(t') = y(t', \alpha) \quad (\text{III.7})$$

where

$$y(t', \alpha) \equiv \pm \frac{1}{vV} (\alpha - t' \mp V)$$

is a straight line and $\tau(t')$ is a saw-shape function plotted in Fig.10. The plot shows two cases in dependence on the sign of the boost velocity u .

Due to periodicity of the oscillon the parameter α is restricted to the interval $0 \leq \alpha < 1$. This can be seen from Fig.8(b) (case $u = +V$), where the simultaneity lines $t = 0$ and $t = \gamma$, parallel to the axis x , cross the left border of the oscillon at $(t', x') = (0, 0)$ and $(t', x') = (1, 0)$ and therefore two oscillons seen in the laboratory frame S at the instants of time $t_0 = 0$ and $t_0 = \gamma$ have the same shape. The same is true for $u = -V$ case.

Two straight lines $y(t', \alpha)$ with $\alpha = 0$ and $\alpha = 1$, plotted in Fig.10(a), cross the axis t' at $t' = -V$ and $t' = 1 - V$. Similarly, in the case $u = -V$ they cross the axis t' at $t' = V$ for $\alpha = 0$ and $t' = 1 + V$ for $\alpha = 1$, see Fig.10(b). In order to cover whole range of velocities $V \in [0, 1]$ we shall consider the equation (III.7) on the interval $-1 < t' < 1$ for $u = +V$ and on the interval $0 < t' < 2$ for $u = -V$. The saw-shape function $\tau(t')$ is given by pieces of straight lines $\tau(t') = at' + b$, where

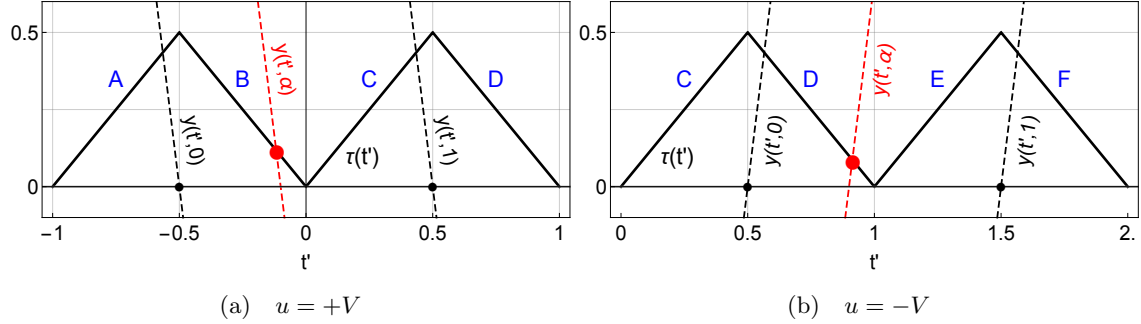


FIG. 10: Functions $\tau(t')$ and $y(t', \alpha)$ for $V = 0.5$ and $v = 0.3$ (here $V > V_c = \frac{10}{23}$). The middle dashed line represents solution of equation (III.7) with certain α ; here $\alpha = 0.4$.

the coefficients (a, b) depend on the value of the coordinate t' , namely

$$(a, b) = \begin{cases} (1, 1) & \text{for } t' \in (-1, -\frac{1}{2}) & (A) \\ (-1, 0) & \text{for } t' \in (-\frac{1}{2}, 0) & (B) \\ (1, 0) & \text{for } t' \in (0, \frac{1}{2}) & (C) \\ (-1, 1) & \text{for } t' \in (\frac{1}{2}, 1) & (D) \\ (1, -1) & \text{for } t' \in (1, \frac{3}{2}) & (E) \\ (-1, 2) & \text{for } t' \in (\frac{3}{2}, 2) & (F) \end{cases}.$$

There are two different cases dependently on an absolute value of the boost velocity $V = |u|$. They are separated by the critical case with velocity

$$V_c \equiv \frac{1}{2+v}.$$

The straight line $y(t', \alpha)$ crosses maxima of $\tau(t')$ i.e. $\tau(t'_{max}) = \frac{1}{2}$ at $t'_{max} = \{-\frac{1}{2}, \frac{1}{2}\}$ for $u = +V$ and at $t'_{max} = \{\frac{1}{2}, 1\}$ in the case $u = -V$. It crosses the minimum $\tau(t'_{min}) = 0$ at $t'_{min} = 0$ for $u = +V$ and at $t'_{min} = 1$ for $u = -V$. The corresponding values of the parameter α are denoted by $\alpha_l^{(\pm)}$ for lower maximum, $\alpha_u^{(\pm)}$ for upper maximum and $\alpha_0^{(\pm)}$ for the minimum. The signs “ \pm ” correspond with $u = \pm V$. They have the form

$$\begin{aligned} \alpha_l^{(+)} &= \frac{1}{2}[-1 + V(2 + v)], & \alpha_l^{(-)} &= \frac{1}{2}[1 - V(2 + v)], \\ \alpha_0^{(+)} &= V, & \alpha_0^{(-)} &= 1 - V, \\ \alpha_u^{(+)} &= \frac{1}{2}[1 + V(2 + v)], & \alpha_u^{(-)} &= \frac{1}{2}[3 - V(2 + v)]. \end{aligned} \quad (\text{III.8})$$

When the boost velocity takes the critical value $V = V_c$ then the lowest value $\alpha = 0$ corresponds with $\alpha_l^{(\pm)}$ and the highest value $\alpha = 1$ with $\alpha_u^{(\pm)}$. Thus only two intervals (B) and (C) for $u = +V$ and (D) and (E) for $u = -V$ are relevant in this case. The interval (D) is covered by α such that $0 \leq \alpha \leq \alpha_0^{(\pm)}$ and (E) is covered by α which satisfies $\alpha_0^{(\pm)} \leq \alpha < 1$. The upper letter stands for upper sign (+) and the lower one for (-).

When the boost velocity is less than the critical value, $V < V_c$, then the straight line $y(t', \alpha = 0)$ crosses the saw-shape chain $\tau(t')$ at certain point given by t' belonging to the interval (D) and $y(t', \alpha = 1)$ crosses the chain $\tau(t')$ at the point with t' that belongs to (F) . Thus in this case the

relevant intervals are $(\frac{B}{D})$, $(\frac{C}{E})$ and $(\frac{D}{F})$. The parameter α takes values $0 \leq \alpha \leq \alpha_0^{(\pm)}$ in the interval $(\frac{B}{D})$, it takes values $\alpha_0^{(\pm)} \leq \alpha \leq \alpha_u^{(\pm)}$ in $(\frac{C}{E})$ and values $\alpha_u^{(\pm)} \leq \alpha < 1$ in $(\frac{B}{F})$. Note that the intervals $(\frac{B}{D})$ and $(\frac{D}{F})$ are covered only partially by α .

On the other hand, for $V > V_c$ (the case sketched in Fig.10) the relevant intervals are $(\frac{A}{C})$, $(\frac{B}{D})$ and $(\frac{C}{E})$. In the interval $(\frac{A}{C})$ the parameter α belongs to $0 \leq \alpha \leq \alpha_l^{(\pm)}$, in $(\frac{B}{D})$ it belongs to $\alpha_l^{(\pm)} \leq \alpha \leq \alpha_0^{(\pm)}$ and in $(\frac{C}{E})$ it belongs to $\alpha_0^{(\pm)} \leq \alpha < 1$. In this case the intervals $(\frac{A}{C})$ and $(\frac{C}{E})$ are covered only partially by α .

The solution of the equation (III.7) is given by

$$t'(\alpha) = \frac{\alpha \mp V(1 + bv)}{1 \pm avV} \quad (\text{III.9})$$

where the values of (a, b) are determined by the velocity V and the phase α . A position of the right endpoint of the oscillon, determined from the spacetime interval, reads

$$x_0(\alpha) = \sqrt{\gamma^2 \alpha^2 - t'(\alpha)^2 + x'^2},$$

where x' introduced in (III.6) is a function of α given by $x'(\alpha) = 1 + v \left(at'(\alpha) + b \right)$. After some manipulations one gets

$$x_0(\alpha) = \frac{\gamma}{1 \pm avV} \left[(1 - V^2)(1 + vb) + \alpha(\pm V + va) \right]. \quad (\text{III.10})$$

This results shows that x_0 is a linear function of α in the intervals in which (a, b) remain constant functions of α .

Now we shall determinate the function $\tilde{x}_0(\alpha)$ which describes position of *left endpoint* of the oscillon. The left border of the oscillon corresponds with the world-line $x' = v\tau(t')$ in the rest frame of the oscillon. In order to determine the coordinate $t'(\alpha)$ one has to solve equation

$$\tau(t') = z(t', \alpha) \quad \text{where} \quad z(t', \alpha) = \pm \frac{\alpha - t'}{vV}.$$

Plugging $\tau(t') = a't' + b'$ we find that $t'(\alpha)$ is given by

$$t'(\alpha) = \frac{\alpha \mp b'vV}{1 \pm a'vV}.$$

The coefficients (a', b') correspond with $0 \leq t' \leq \frac{1}{2}$ and $\frac{1}{2} \leq t' < 1$ and they read

$$(a', b') = \begin{cases} (1, 0) & \text{for } 0 \leq t' \leq \frac{1}{2} \quad (C) \\ (-1, 1) & \text{for } \frac{1}{2} < t' < 1 \quad (D) \end{cases}$$

We denote solutions of the equation $\tau(t'_{\max}) = \frac{1}{2}$ by $\alpha_c^{(\pm)}$. They read

$$\alpha_s^{(\pm)} := \frac{1}{2}(1 \pm vV).$$

For $0 \leq \alpha \leq \alpha_s^{(\pm)}$ the line $z(t, \alpha)$ crosses $\tau(t')$ at (C) and for $\alpha_s^{(\pm)} \leq \alpha < 1$ it crosses $\tau(t')$ at (D). Taking similar steps as for the case of right endpoint we find

$$\tilde{x}_0(\alpha) = \frac{\gamma}{1 \pm a'vV} \left[(1 - V^2)(vb') + \alpha(\pm V + va') \right]. \quad (\text{III.11})$$

5. Remarks on initial configurations

Having expressions for $x_0(\alpha)$ and $\tilde{x}_0(\alpha)$ we can construct arbitrary configurations containing oscillons which begin to collide at $t = 0$. In the case of oscillons with $|u| < v$ an additional caution is necessary. In Fig.11 we show worldsheet of two oscillons which form symmetric configuration

$$\Psi^{(s)}(t, x) = \psi(t + \alpha\gamma, x + x_0(\alpha); v, V) + \psi(t + \alpha\gamma, -x + x_0(\alpha); v, V)$$

and the field configuration $\Psi^{(s)}(x) = \Psi^{(s)}(t, x)|_{t=0}$, $\Psi_t^{(s)}(x) = \partial_t \Psi^{(s)}(t, x)|_{t=0}$ with $|u| < v$. Fig.11(b) shows that for some values of phase of colliding oscillons they collide *before* the instant of time $t = 0$. It means that corresponding configuration $(\Psi^{(s)}(x), \Psi_t^{(s)}(x))$ cannot be obtained by

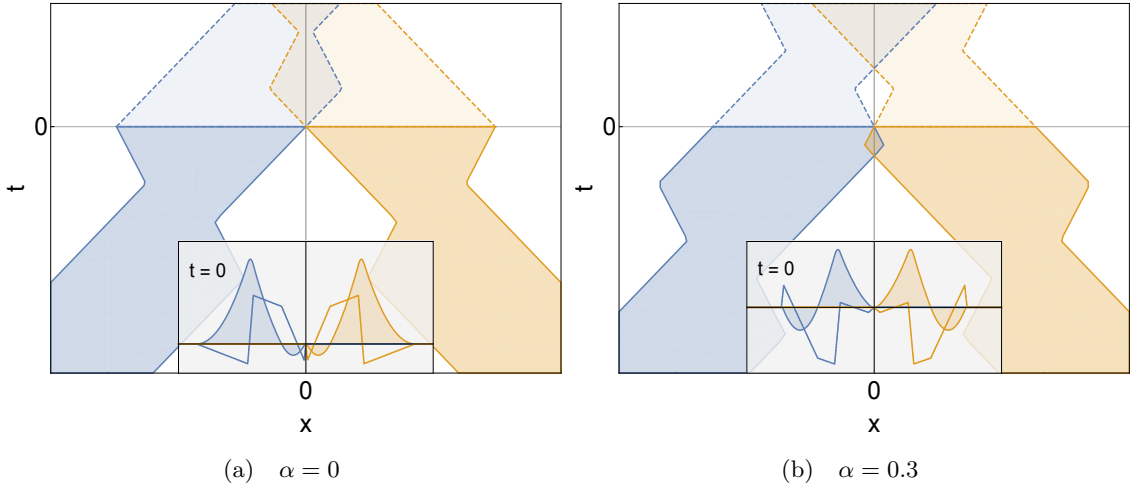


FIG. 11: Symmetric configurations with $v = 0.8$ and $V = 0.5$ and different phases.

approach of two travelling oscillons. A requirement that worldsheets of colliding oscillons have no intersections for $t < 0$ excludes such field configurations.

Although we put main attention to symmetric (antisymmetric) initial configurations it is quite straightforward that nonsymmetric configurations with vanishing total momentum can be obtained taking different phase for each colliding oscillon. An example of two oscillons with phases α_L and α_R given by

$$\Psi(t, x) = \psi(t + \alpha_L\gamma, x + x_0(\alpha_L); v, V) + \psi(t + \alpha_R\gamma, -x + x_0(\alpha_R); v, V) \quad (\text{III.12})$$

is shown in Fig.12(a). This field configuration is obtained by shifting the first oscillon by distance $x_0(\alpha_L)$ (placing it to the left of $x = 0$) and the second one by $x_0(\alpha_R)$ and reflection $x \rightarrow -x$ (placing it to the right of $x = 0$). Another possibility is shown in Fig. 12(b). The first oscillon, with $u = -V$, is shifted by $\tilde{x}_0(\alpha_R)$ (which places it to the right of $x = 0$) and the second oscillon, with $u = +V$, is shifted by $x_0(\alpha_L)$ (which places it to the left of $x = 0$). In this case

$$\Psi(t, x) = \psi(t + \alpha_R\gamma, x + \tilde{x}_0(\alpha_R); v, -V) + \psi(t + \alpha_L\gamma, x + x_0(\alpha_L); v, V).$$

It is quite clear from diagrams in Fig.12 that there exist set of phases that worldsheet of oscillons overlap for $t < 0$.

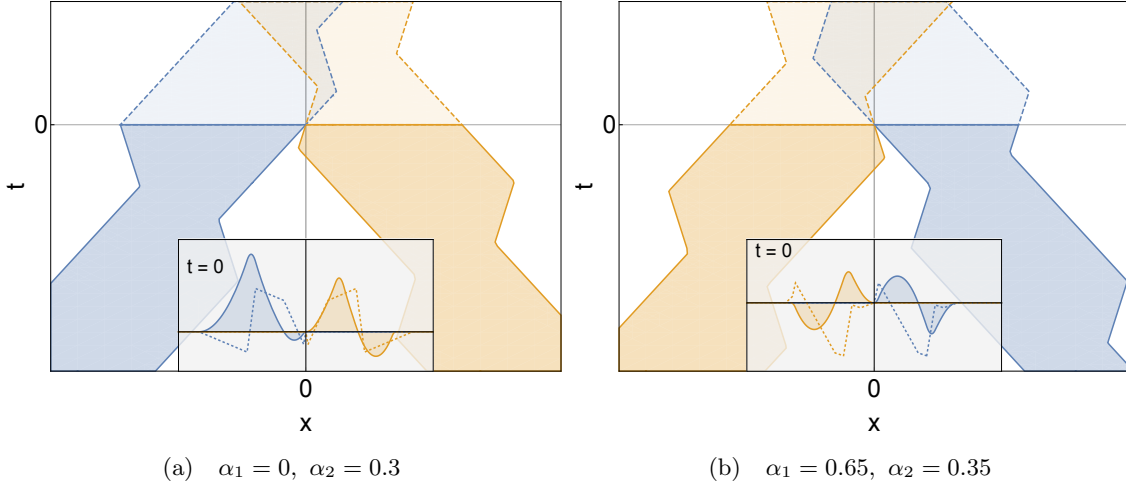


FIG. 12: Generic configurations with $v = 0.7$ and $V = 0.5$. (a) shift by right endpoint, (b) shift by left endpoint.

B. Antisymmetric configurations

In this section we shall present some numerical results for scattering of two oscillons which form an antisymmetric initial configuration of the signum-Gordon field. We have chosen antisymmetric initial data to be studied at first because the result of scattering of oscillons in such a case is relatively low when comparing with results obtained for symmetric configurations. The fact that initial configuration is antisymmetric implies that it must hold

$$\Psi^{(a)}(t, x; v, V)|_{x=0} = 0 \quad (\text{III.13})$$

for any instant of time t . This condition expresses vanishing of the net force exercised on a degree of freedom at $x = 0$ (*e.g.* ball, pendulum in a discretized mechanical realization of the model). In other words, the only effect of interaction between left and right oscillon is a fixing of the value of scalar field $\chi = 0$ at $x = 0$. Thus the evolution of the system in regions $x < 0$ and $x > 0$ effectively splits into two independent problems containing an initial oscillon and the boundary condition (III.13).

In our numerical study we have evolved an antisymmetric configuration without assuming that $\chi = 0$ at $x = 0$. Looking at results presented in Fig.13 we clearly see that the condition (III.13) is satisfied. It manifests itself in the presence of a vertical white segments at $x = 0$. Another important observation is the absence of radiation in the central region of the diagram independently on the value of initial speed of oscillons. The sources of radiation generated in this process are irregular borders of two outgoing oscillons, see Fig.13(a).

One can note that irregularities of the border appear likely for small velocities V of colliding oscillons than for higher ones. Moreover, in spite of being irregular the outgoing oscillons radiate significantly less than it would be expected for strongly perturbed oscillons. In fact, the outgoing oscillons with irregular borders belong to more general class of oscillons. We address Sec.III E to a discussion of this subject.

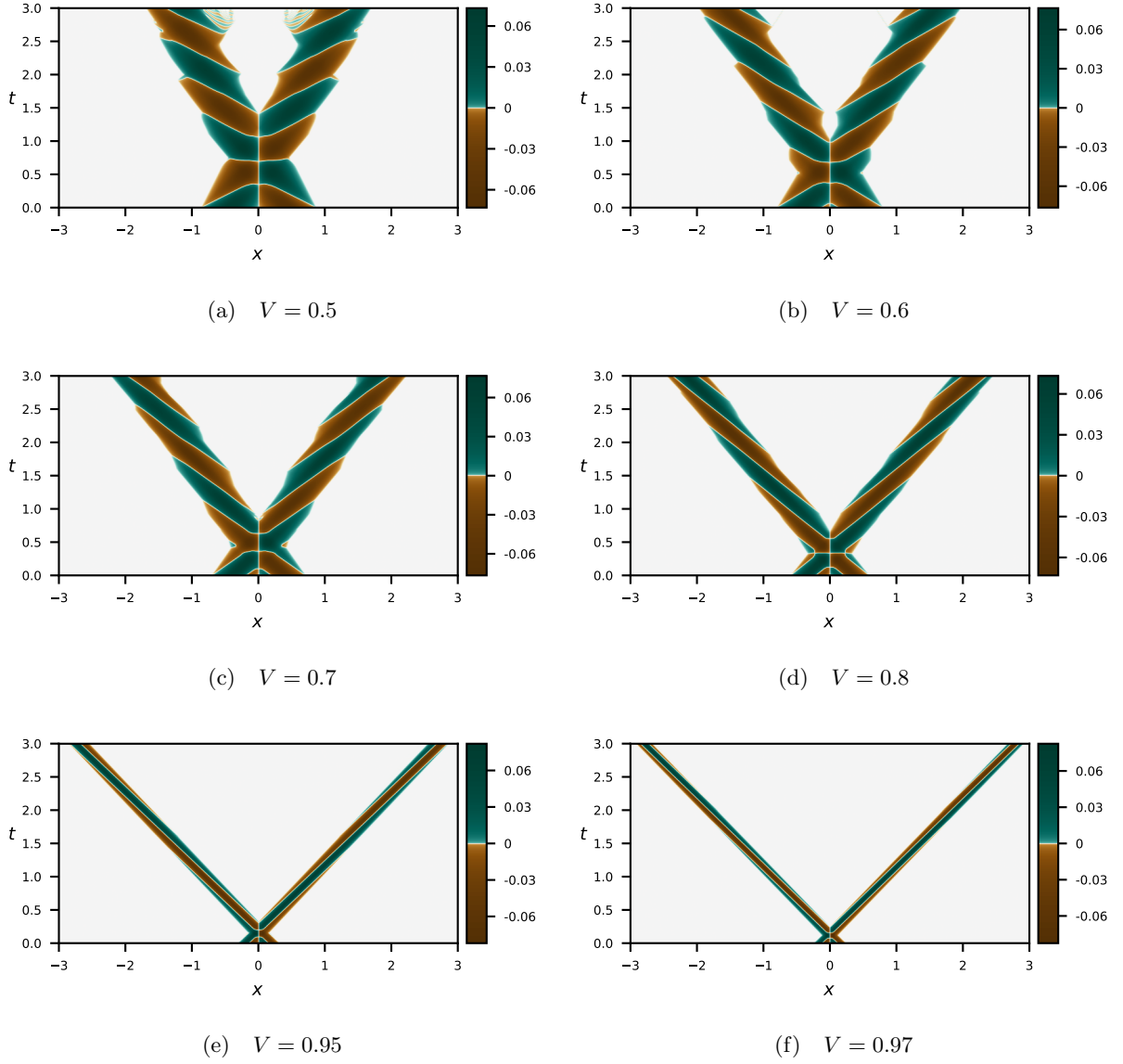


FIG. 13: The scattering of oscillons (antisymmetric configuration) in dependence on their initial speed V . The initial configuration contains oscillons with phase $\alpha = 0$ and no zig-zag motion of their border.

Another interesting question is the dependence of the scattering process on the phase α that characterizes the initial configuration. In Fig.14 we present the result of scattering for $V = 0.8$ and four values of the phase. The figures show very similar evolution of initial configurations that differ by the value of parameter α .

Another parameter that the incoming oscillons depend on is the speed v of the oscillon border in its rest frame. Numerics shows that irregularities of borders of two outgoing oscillons increase with increasing of the value of parameter v which determine the swaying motion of incoming oscillons. in Fig.15 we show results of scattering of anti-symmetric configuration of oscillons with speed $V = 0.8$, phase $\alpha = 0$ and speed of the border $v = 0.47$ and $v = 0.82$. The figures show that as borders of outgoing oscillons became more and more irregular the the number and size of oscillons

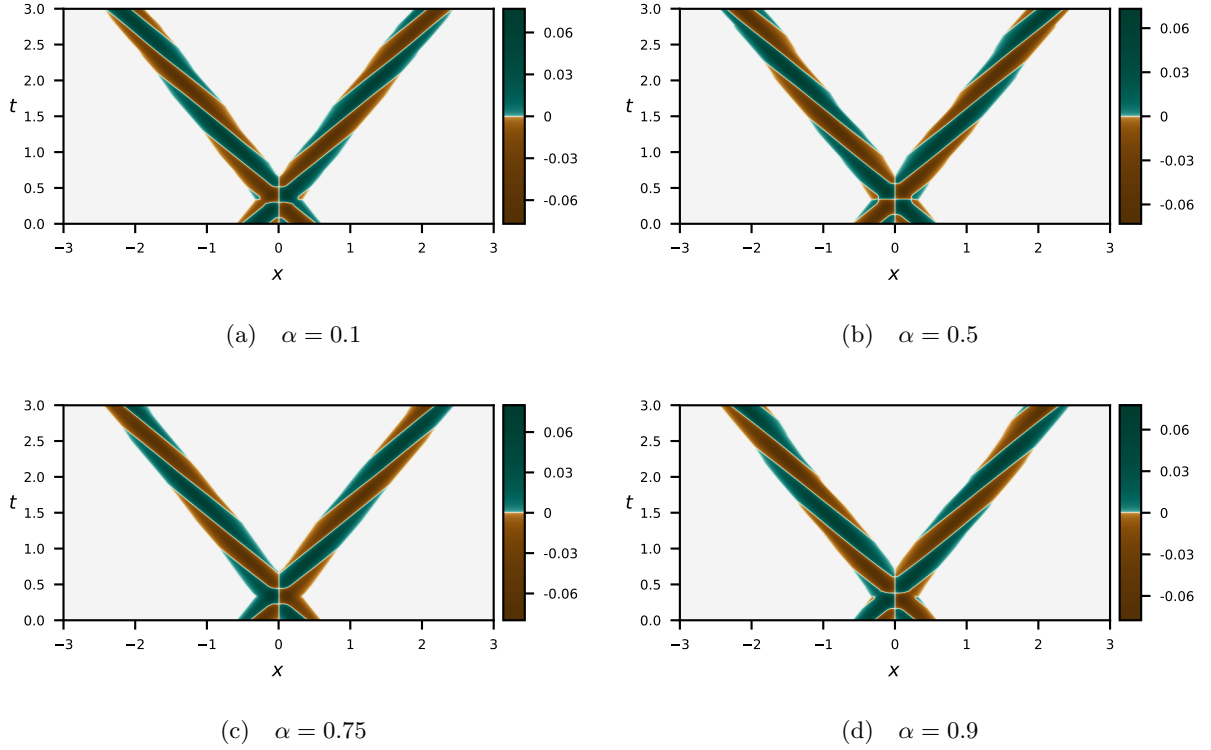


FIG. 14: The scattering of oscillons (antisymmetric configuration) in dependence on their phase α . The initial configuration contains oscillons with speed $V = 0.8$ and no zig-zag motion of their border.

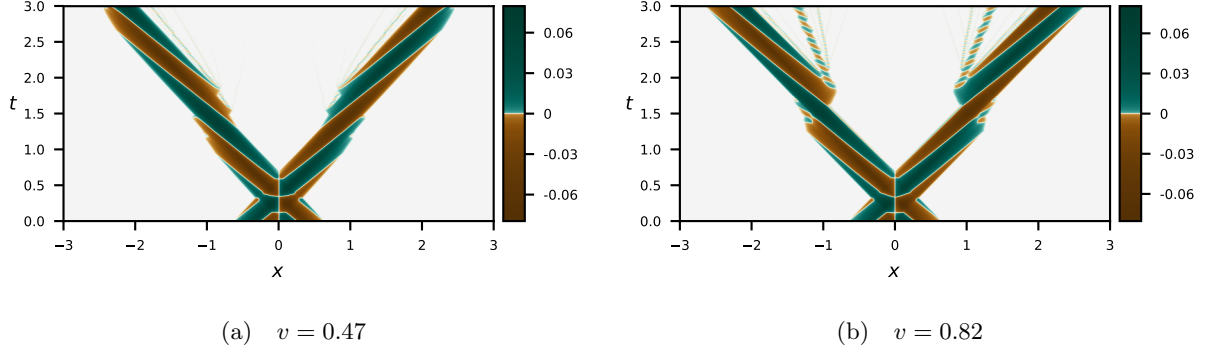


FIG. 15: The scattering of oscillons (antisymmetric configuration) in dependence on parameter v . The initial configuration contains oscillons with speed $V = 0.8$ and $\alpha = 0$.

emitted from these borders increases.

It is quite notable that radiation generated in the process of scattering of anti-symmetric configurations is emitted only from irregularities of borders of outgoing oscillons. Such oscillons can be interpreted as (strongly) perturbed exact oscillons of the signum-Gordon model. The surplus of their energy is converted into small oscillons which are sent away from irregularities.

C. Symmetric configurations

1. Overview of the numerical results

In this section we present a general overview of numerical solutions for symmetric initial configurations parametrized by boost velocity V , initial phase α . For better transparency we shall present first only the cases with $v = 0$. They are sufficient to give a basic notion about typical results of the scattering. In section [III C 4](#) we give further examples of oscillons with non-zero velocity of the border v .

A typical situation with $v = 0$ is shown in Fig.16. Two incoming oscillons form the initial configuration at $t = 0$. This configuration is adopted as an input for numerical simulation.

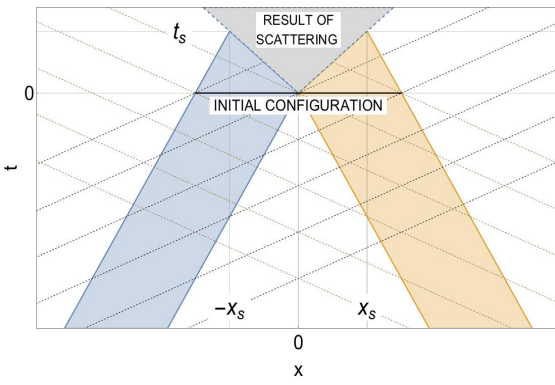


FIG. 16: Worldsheets of two incoming oscillons for $v = 0$. The oscillons are unperturbed inside two triangular regions above the line $t = 0$. The zeros of the oscillon correspond with intersections of its worldsheet with a family of dashed lines.

We performed many numerical simulations for distinct velocities and phases of scattered oscillons. In Fig.17 we plot the scattering process of two oscillons with $v = 0$ and $\alpha = 0$ for six values of boost velocity V . All initial configurations contain two oscillons whose supports touch each other at $t = 0$. Numerics shows that the result of collision strongly depends on the velocity V of colliding oscillons. All six diagrams contain two oscillon-like objects (perturbed oscillons) that emerge shortly after collision. They move with velocity which is almost equal to velocity of colliding oscillons. The emerging oscillon-like objects obtained in the process of scattering are significantly less regular when initial velocities of oscillons are small. A fundamental difference between diagrams is visible in their central region where there appears radiation which takes the form of jets. Looking more carefully at the radiation we see that it contains certain structures that strongly resemble oscillon-like objects. Note also that emerging oscillons obtained for small velocities V emit similar oscillon-like objects directly from their irregular border. A presence of the radiation in the scattering process reflects a non-integrable character of the signum-Gordon model.

In Fig.18 we present numerical results of scattering of two oscillons with $V = 0.93$, $v = 0$ and four initial phases $\alpha = 0$, $\alpha = 0.25$, $\alpha = 0.84$ and $\alpha = 0.93$. The figure indicates that the initial phase of colliding oscillons is indeed a relevant scattering parameter. The form of jets in each

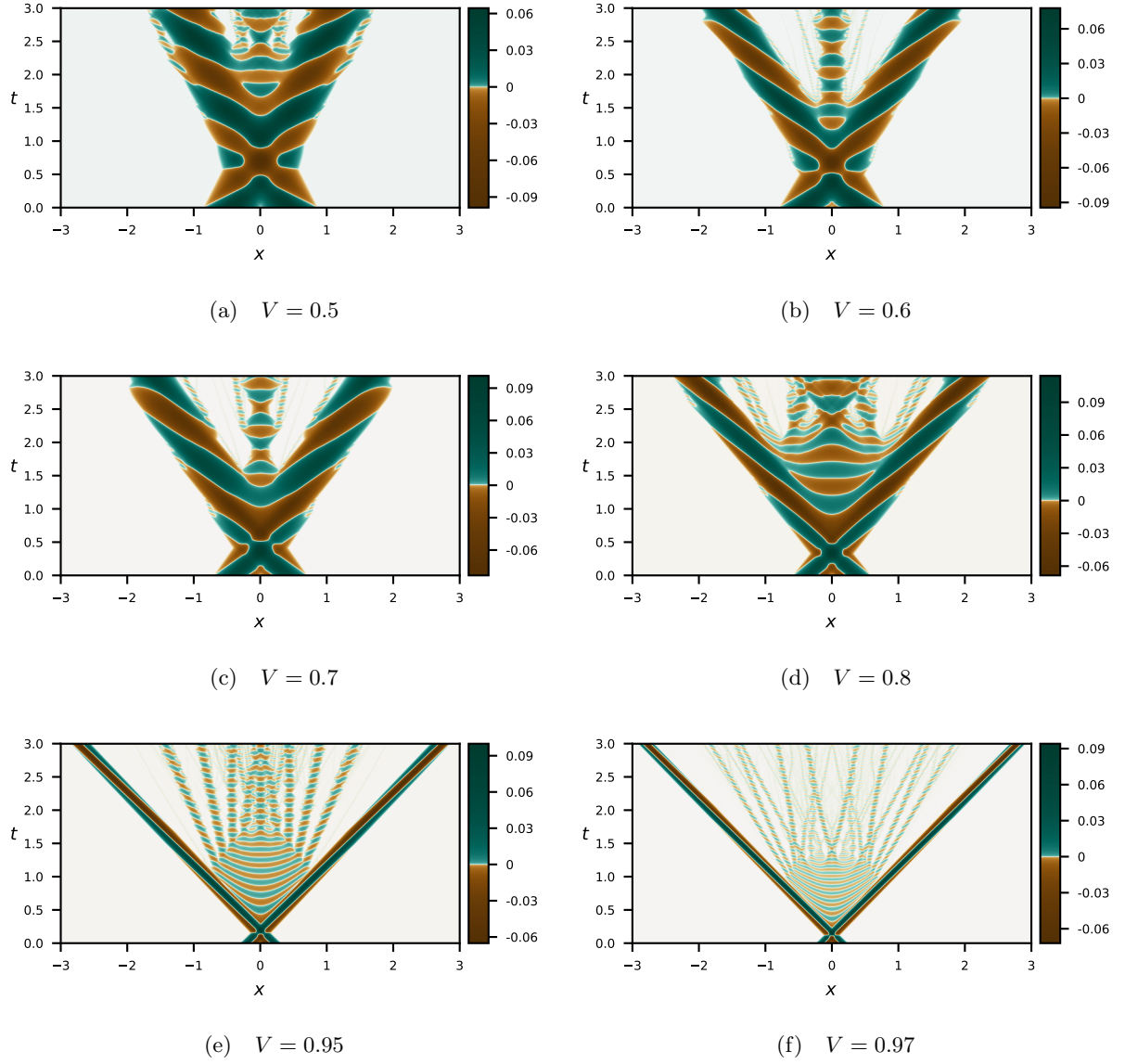


FIG. 17: The scattering of oscillons (symmetric configuration) in dependence on their initial speed V . The initial configuration contains oscillons with phase $\alpha = 0$ and no zig-zag motion of their border $v = 0$.

subfigure of Fig.18 is clearly different. It shows that the result of scattering process is very sensible on the value of the phase α .

Looking at figures Fig.17 and Fig.18 we see that in the first stage of scattering the interacting oscillons exist on support that shrinks from its initial size $2L$ to certain minimal size $2L_{\min}$ where $L = \sqrt{1 - V^2}$ is the size of the oscillon in the laboratory reference frame. This process takes some time t_s . For $t > t_s$ we observe emerging of two leading oscillons and appearance of waves of energy which we call radiation. In order to evaluate the time t_s we assume that left (right) border of the oscillon that moves with $u = V$ ($u = -V$) moves freely with the velocity that the oscillon have in the laboratory reference frame until it hits the future light cone of the event $(0, 0)$; see Fig.16. This assumption allows to determine the event P_s with the coordinates (t_s, x_s) in the laboratory

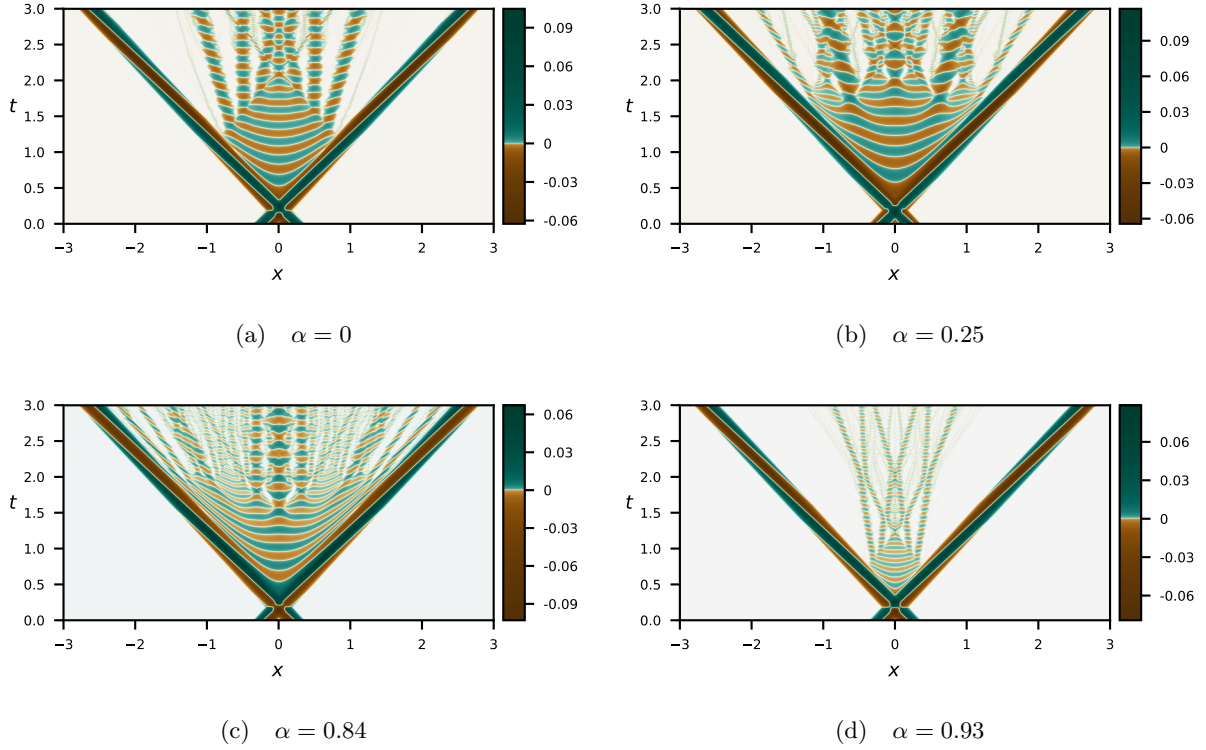


FIG. 18: The scattering process for initial symmetric configuration containing oscillons with speed $V = 0.93$ and no zig-zag motion of their border and different initial phases α .

reference frame. Thus the left border of the left oscillon is given by $x = -\sqrt{1 - V^2} + Vt$ and it intersects the light cone line $x = -t$ at

$$t_s = \sqrt{\frac{1 - V}{1 + V}} = -x_s. \quad (\text{III.14})$$

The formula (III.14) is valid exclusively for $v = 0$. Due to symmetry of the initial configuration we see that the minimal support size of the scattering oscillons can be estimated by expression $\Delta x_{\min} = 2\sqrt{\frac{1-V}{1+V}}$. In Fig.19 we show numerical data (dots) and analytical curves (solid lines) representing the characteristic time of scattering t_s and the minimum size of the oscillon configuration Δx_{\min} at t_s .

2. High velocities - formation of shock waves

Let us look in more detail on some of our numerical results. For small velocities the numerical solution is very irregular. Looking at figures Fig.17(a)-(c) we clearly see a formation of strongly perturbed oscillon with center at $x = 0$. This oscillon is unstable and irradiates smaller oscillons. The situation changes for high velocities for which the numerical solution consists on regular patterns. In particular, when velocity of oscillons is close to unity another interesting solution emerges. An example of such a solution is presented in Fig.17(e). The solution presented there was obtained for scattering of two oscillons with initial phase $\alpha = 0$, speeds $V = 0.93$ and no

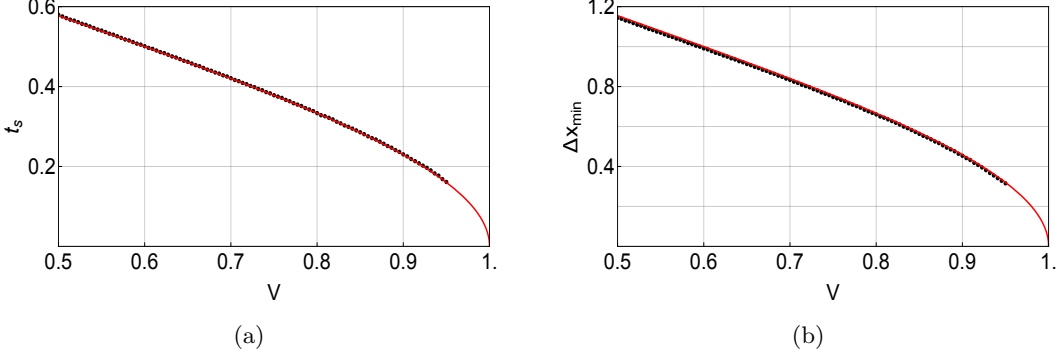


FIG. 19: The cases of different velocities V . (a) Characteristic time t_s and (b) the minimum size Δx_{\min} . Dots represent numerical data whereas solid curves stand for expressions $t_s = \sqrt{\frac{1-V}{1+V}}$ and $\Delta x_{\min} = 2t_s$.

swaying motion *i.e.* for $v = 0$. A very characteristic feature of the solution is a presence of regular waves that are localized in a diamond-shape region on the Minkowski diagram. Such waves emerge shortly after collision and eventually decay in a sequence of oscillon-like structures. It turns out that the nature of these waves can be understood in terms of so-called *shock waves* that are exact solutions of the signum-Gordon model reported in [35].

The shock wave is a particular class of solutions of the signum-Gordon model with two discontinuities that propagate with the speed of light. Here we do not observe such wavefronts due to presence of two oscillons that move with subluminal velocities. The collapse of the wave suggests that our numerical solution is only a good approximation of the exact shock wave which would exist for arbitrary times $t > 0$.

We check the hypothesis about the nature of the wave solution comparing their zeros with zeros of analytical shock wave. According to [35] the shock wave solutions is a class of the signum-Gordon solution given by $\phi(t, x) = \theta(-z)W(z)$, where $z = \frac{1}{4}(x^2 - t^2)$. The function $W(z)$ obeys the ordinary equation $zW''(z) + W'(z) = \text{sgn}(W(z))$ and it consists of infinitely many partial solutions $W_k(z)$, $k \in \mathbb{Z}$ matched at points $-a_k$. Each partial solution satisfy equation $zW_k''(z) + W_k'(z) = (-1)^k$ and the conditions $W_k(-a_k) = 0 = W_{k+1}(-a_k)$ and $W_k'(-a_k) = W_{k+1}'(-a_k)$. It can be written in the form

$$W_k(z) = (-1)^k \left(z + a_k + b_k \ln \frac{|z|}{a_k} \right)$$

where

$$\frac{b_{k+1}}{a_k} = 2 - \frac{b_k}{a_k}, \quad \text{and} \quad \frac{a_{k+1}}{a_k} = 1 + \frac{b_{k+1}}{a_k} \ln \frac{a_{k+1}}{a_k}. \quad (\text{III.15})$$

Note that $b_0 = 0$ in order to avoid singularity of the logarithm at $z = 0$. The first zero a_0 is a free parameter which determines values of all other constants via recurrence relations (III.15). In particular $b_1 = 2a_0$. Denoting $\alpha_{k+1} := \frac{1}{2} \frac{b_{k+1}}{a_k}$ and $y_{k+1} := \frac{a_{k+1}}{a_k}$ one gets relations (III.15) in the form

$$\alpha_{k+1} = 1 - \frac{\alpha_k}{y_k}, \quad \text{and} \quad y_{k+1} = 1 + 2\alpha_{k+1} \ln y_{k+1}. \quad (\text{III.16})$$

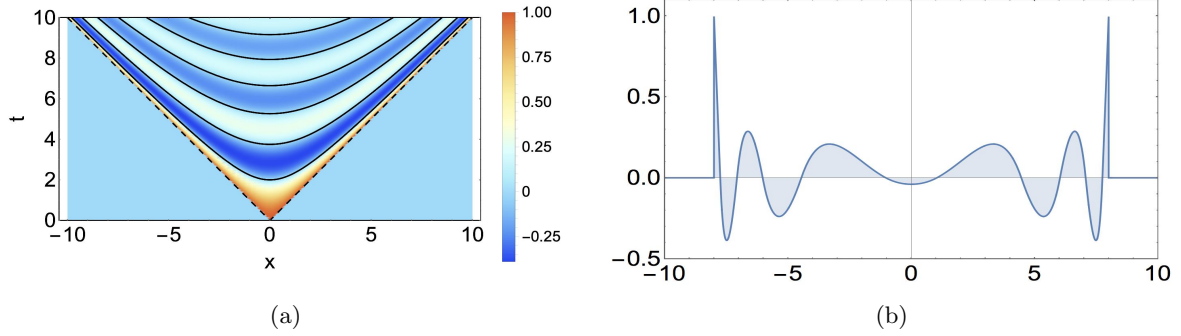


FIG. 20: The exact shock wave solution for $a_0 = 1$. (a) The solution on the space-time diagram and (b) the snapshot of the solution for $t = 8.0$.

Note that $\alpha_1 = 1$. It follows from (III.16) that α_{k+1} is determined by a_k and b_k . Solving numerically the second equation of (III.16) one gets y_{k+1} and so a_{k+1} and b_{k+1} can be determined. The zeros of the field $\phi(t, x)$ are localized on hyperbolas

$$x_k(t) = \pm \sqrt{t^2 - 4a_k}, \quad (\text{III.17})$$

at the spacetime diagram. Such zeros are sketched in Fig.20(a).

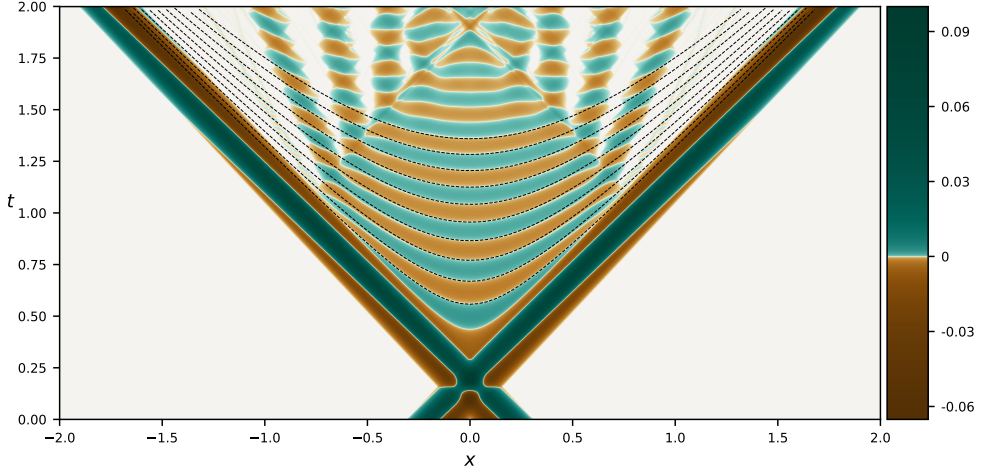


FIG. 21: Scattering of two oscillons for symmetric configuration of the field. The oscillons moves with the speed $V = 0.95$ in the laboratory reference frame. The diamond-shaped structure in the middle resembles the shock wave solution. The fit of ten first zeros was obtained for $a_0 = 0.00541$ and $T_0 = 0.282$.

Having already the analytical form of zeros one can fit the zeros to the numerical data presented in Fig.21. In the process of scattering of two oscillons the formation of waves starts not at $t = 0$ but at some further instant of time T_0 . For this reason the fitting requires, besides a_0 , a second parameter: a time translation T_0 . Thus $x_k(t) = \pm \sqrt{(t - T_0)^2 - 4a_k}$. The trajectories of zeros of exact shock wave solution reproduce very well trajectories of our numerical solution. It supports our hypothesis about shock wave character of regular oscillations localized in the diamond-shape region of Fig.21. Clearly, the numerical shock-like wave solutions are similar to the exact ones

only in a limited region on the Minkowski diagram. Outside of this region they break and produce oscillon-like structures.

3. Vanishing of radiation

In our numerical study we spotted a very interesting case. Namely, some symmetric initial configurations evolve in the way that the resulting field contains only the main oscillons i.e. the amount of radiation generated in this process is virtually insignificant. This phenomenon was observed in the regime of high velocities (V approximately above 0.7) i.e. when two main outgoing oscillons have quite regular form. We found that there are two phases α associated with given velocity V for which the radiation is absent. Fig.22 shows two examples of the scattering process containing initial configurations with identical velocities $V = 0.93$ and different phases α . We have chosen $v = 0$ for both cases. The phases of configurations shown in Fig.22(a) and Fig.22(b) differ by a factor $\Delta\alpha = 0.5$.

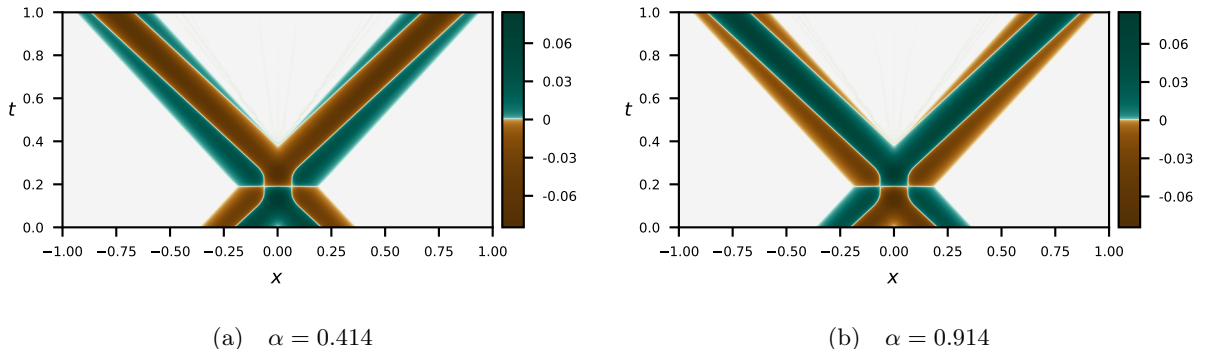


FIG. 22: The scattering result of symmetric initial configuration with $V = 0.93$, $v = 0$. The scattered oscillons have phase (a) $\alpha = 0.414$ and (b) $\alpha = 0.914$.

This difference of phases can be understood comparing the zeros of the incoming oscillons in figures (a) and (b). The initial configurations at $t = 0$ and worldsheets of the oscillons for $t < 0$ were plotted in Fig.23. We have also marked the zeros of the oscillons. They correspond with segments of straight lines

$$x^{(n)}(t) = \frac{t}{V} + B^{(n)}(\alpha), \quad \text{where} \quad B^{(n)}(\alpha) \equiv \frac{\gamma}{2V} \left(2\alpha - \frac{n}{\gamma^2} \right) - x_0(\alpha) \quad (\text{III.18})$$

and where $x_0(\alpha)$ is given by (III.10) and $n = 0, \pm 1, \pm 2, \dots$ stands for numeration of infinite sequence of zeros. Since $x_0(\alpha)$ is a linear function of the phase α then the coefficients $B^{(n)}(\alpha)$ are also linear functions of α . Expression (III.18) shows that all the zeros of the oscillon travel with the same speed equal to $1/V$. Moreover, this expression also shows that two consecutive zeros numbered by n and $n + 1$ lies on the same straight line if phases of these oscillons differ by a certain value $\Delta\alpha$ determined from the equation $B^{(n+1)}(\alpha + \Delta\alpha) - B^{(n)}(\alpha) = 0$ with $v = 0$. This equation has a solution $\Delta\alpha = \frac{1}{2}$. In particular, it means that the incoming zeros $x^{(0)}(t)$, shown in Fig.23(a),

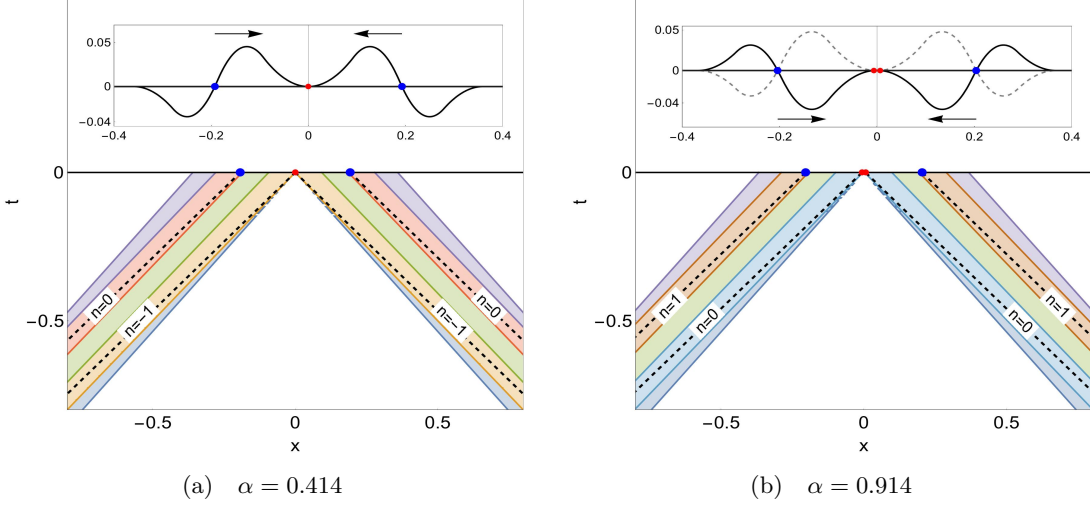


FIG. 23: Initial profile of the signum-Gordon field and worldsheets of the incoming oscillons for $V = 0.93$, $v = 0$ and (a) $\alpha = 0.414$, (b) $\alpha = 0.914$. The zeros are marked by dashed lines. Theirs positions at $t = 0$ are given by (a) $B^{(-1)}(\alpha) = -0.006$, $B^{(0)}(\alpha) = -0.204$ and (b) $B^{(0)}(\alpha) = -0.006$, $B^{(1)}(\alpha) = -0.204$.

and $x^{(1)}(t)$, shown in Fig.23(b), follow on the same straight line. Moreover, it can be checked that both initial configurations characterized by phases α and $\alpha + \frac{1}{2}$ differ only by the sign *i.e.* $\psi \rightarrow -\psi$ when $\alpha \rightarrow \alpha + \frac{1}{2}$, see the insertion plot in Fig.23(b).

The case presented in Fig.22 is not unique. Numerics suggests that in the regime of high velocities V one can fine-tune initial parameters V and α (and also v , see next section) in the way that the outgoing oscillons are not accompanied by radiation. The absence of radiation means that the outgoing oscillon has virtually the same energy as the incoming one. In the most common situations there is certain difference of energies and this difference is released in the form of huge number of small oscillon-like structures. In Fig.24 we plot energy radiated by the system as a fraction of its initial energy. Two dark regions in the upper part of the diagram represent initial parameters (α, V) such that this fraction approaches zero. According to this picture the initial configurations that minimize the radiation have α and V that lie on (approximately) straight line. For $V < 0.7$ the outgoing oscillons are quite irregular; see for instance Fig.17(a). Usually in the vicinity of irregular outgoing oscillons there exists some radiation that originates in these irregularities. For this reason determination of the energy of outgoing oscillons is less reliable for small velocities.

4. Oscillons with $v \neq 0$

In this section we shall present some results of scattering of generalized oscillons *i.e.* oscillons which depend on v – the parameter responsible for swaying motion of the border. In Fig.25 we show wordsheets of two such oscillons. The configuration at $t = 0$ is adopted as initial data for numerical simulation. In similarly to the case $v = 0$ we can obtain expressions for characteristic time of scattering t_s and minimum support size $\Delta x_{\min} = 2|x_s|$ solving equations $x = -L(\alpha) + wt$

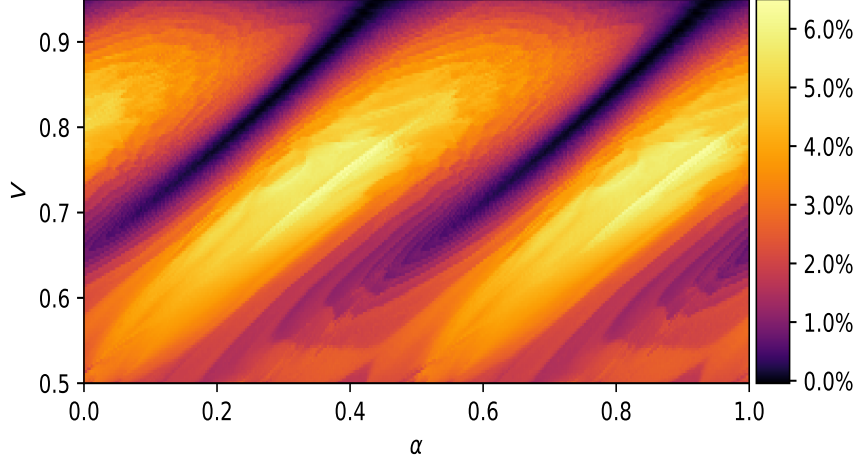


FIG. 24: Fraction of the total energy of initial configuration carried out by radiation for $v = 0$.

and $x = -t$ which gives

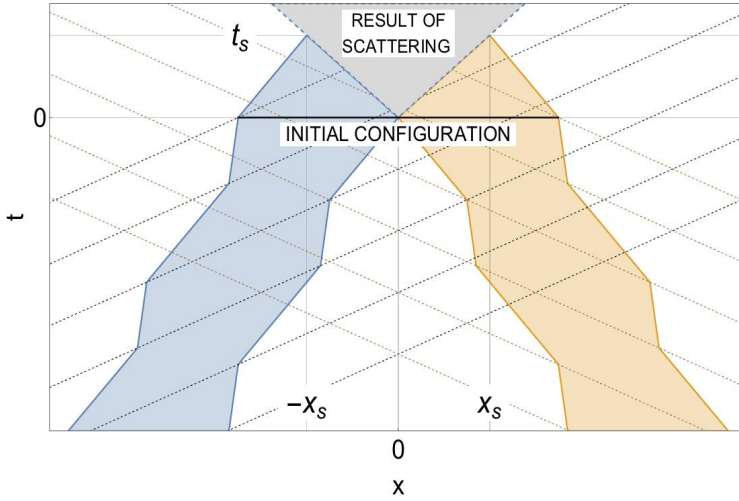


FIG. 25: Worldsheets of two incoming oscillons for $v \neq 0$. The oscillons are unperturbed inside two triangular regions above the line $t = 0$. The zeros of the oscillon correspond with intersections of its worldsheet with a family of dashed lines.

$$t_s = \frac{L(\alpha)}{1+w} = -x_s, \quad \text{where} \quad w \equiv \frac{V+v}{1+Vv} \quad (\text{III.19})$$

and where $L(\alpha) \equiv x_0(\alpha) - \tilde{x}_0(\alpha)$ is the size of the oscillon at $t = 0$. $x_0(\alpha)$ is given by (III.10) and $\tilde{x}_0(\alpha)$ by (III.11).

An interesting question is how the replacement of $v = 0$ by $v \neq 0$ modifies the results of the scattering process. For instance, we can take a $v \neq 0$ generalization of the symmetric initial configuration with $V = 0.93$ and $\alpha = 0.414$. In Fig.26(a) we present the result of the scattering for $v = 0.02$. We see that even such small value of the parameter v is sufficient for appearance of shock waves which further transform into cascade of oscillons. It shows that the scattering process

is quite sensible on the value of the parameter v . In order to minimize this radiation one can adjust properly the parameter α . We have found that in this specific case the radiation vanishes for $\alpha = 0.420$ and $\alpha = 0.918$, see Fig.26(b) and (d). For higher values of v there was much more radiation emitted during the process of scattering.

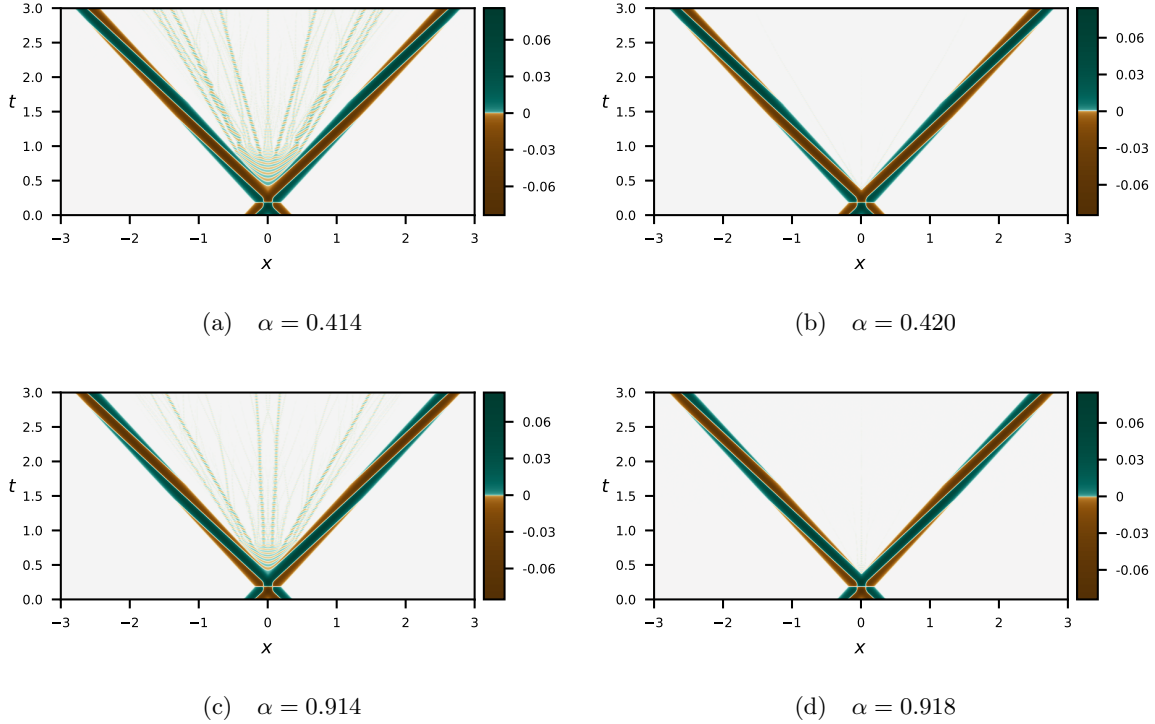


FIG. 26: The scattering process for initial symmetric configuration containing oscillons with speed $V = 0.93$, velocity of the border $v = 0.02$ and different phases α .

In Fig.27 and Fig.28 we present the cases $v = 0.2$ and $v = 0.7$. In both cases we found two values of the phase α that minimize the radiation.

Looking carefully at the initial configurations we see that there is a significant difference between the case $v = 0$ and $v \neq 0$. In Fig.29 we present initial field configurations that minimize the radiation. Comparing configuration $\Psi^{(s)}(x; v, V, \alpha + \Delta\alpha)$, where $\Delta\alpha$ is known from numerics, with $\Psi^{(s)}(x; v, V, \alpha)$ we see that configuration with $\alpha + \Delta\alpha$ is not equal to a negative of the configuration with α . The difference between $\Psi^{(s)}(x; v, V, \alpha + \Delta\alpha)$ and $-\Psi^{(s)}(x; v, V, \alpha)$ increases with increasing of v . On the other hand, $\Psi^{(s)} \rightarrow -\Psi^{(s)}$ is a symmetry of the signum-Gordon equation so if $\Psi^{(s)}(x; v, V, \alpha)$ minimizes the radiation then $-\Psi^{(s)}(x; v, V, \alpha)$ minimizes the radiation as well. Thus, for any set of parameters (v, V) there are four initial configurations $\pm\Psi^{(s)}(x; v, V, \alpha)$ and $\pm\Psi^{(s)}(x; v, V, \alpha + \Delta\alpha)$ that minimize radiation. They are degenerated (there are only two configurations) for $v = 0$.

In Fig.30 we plot the fraction of the initial energy carried by oscillons radiated by the system. The figure was obtained for $v = 0.45$. The dark regions, corresponding with very low value of radiated energy, are less regular when comparing with Fig.24 for the case of vanishing v .

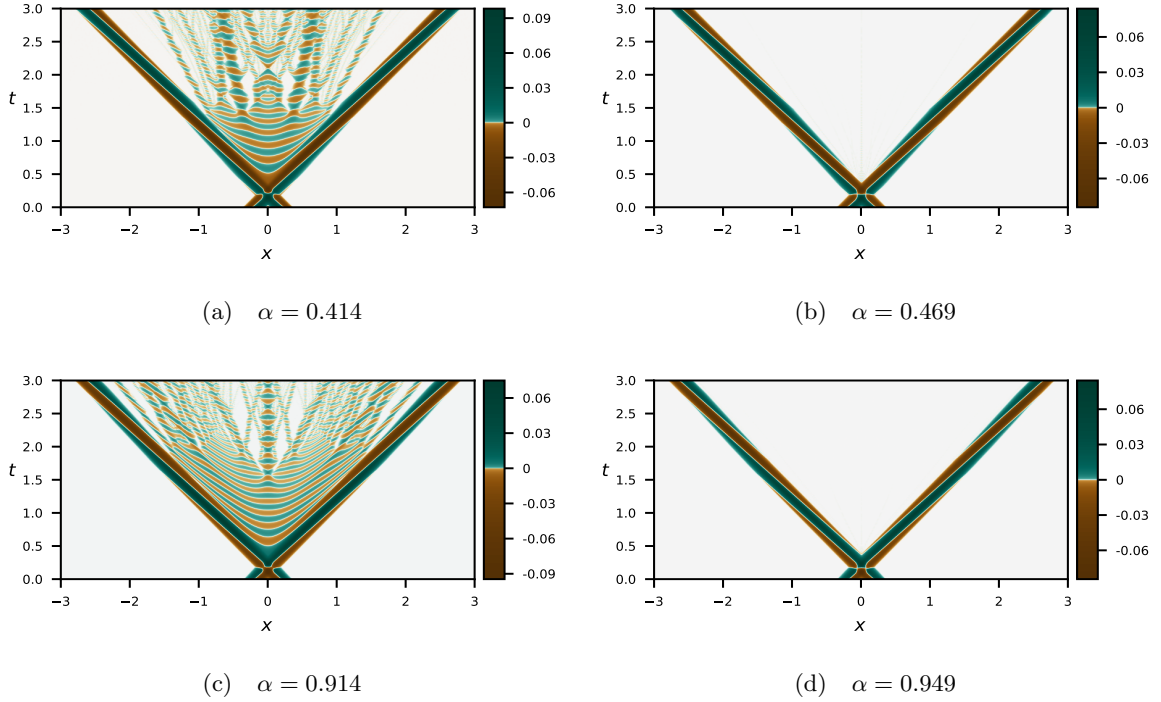


FIG. 27: The scattering process for initial symmetric configuration containing oscillons with speed $V = 0.93$, velocity of the border $v = 0.2$ and different phases α .

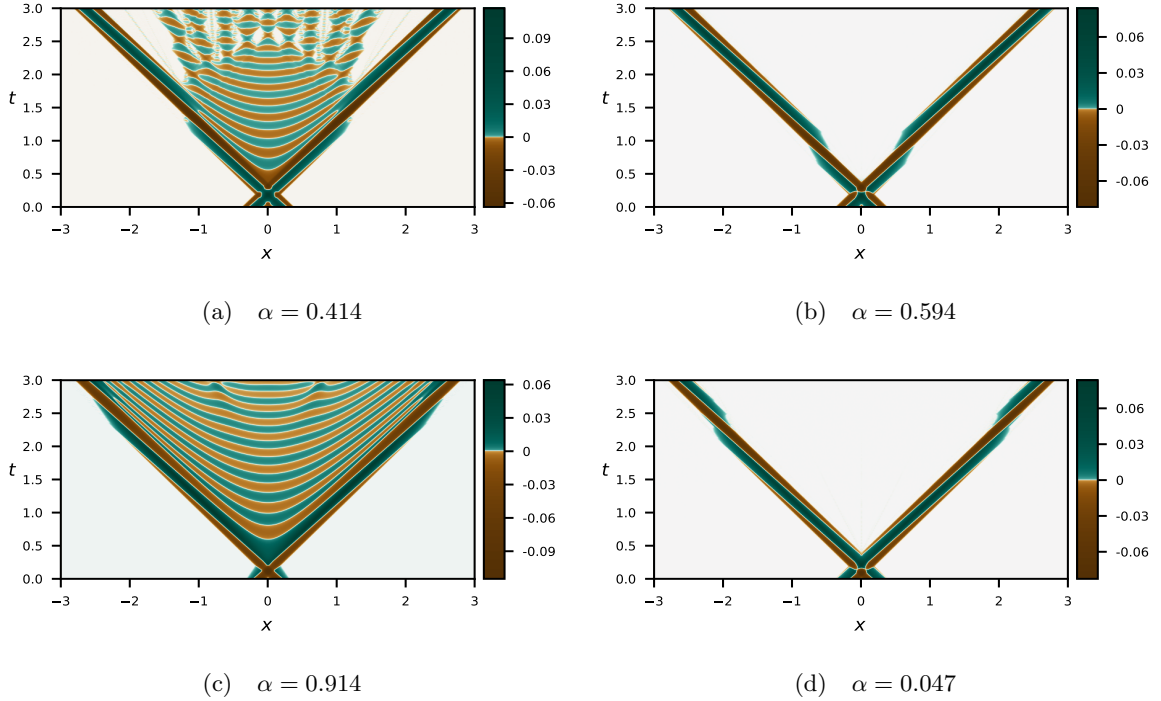
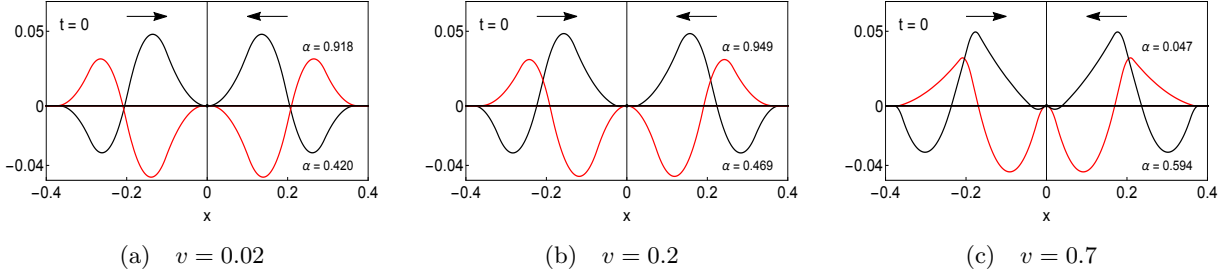
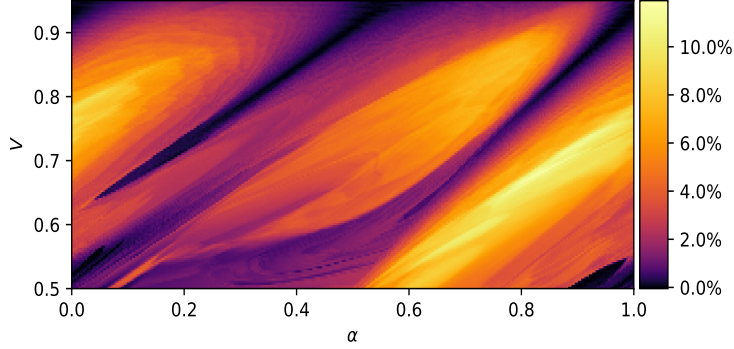


FIG. 28: The scattering process for initial symmetric configuration containing oscillons with speed $V = 0.93$, velocity of the border $v = 0.7$ and different phases α .

FIG. 29: Initial configurations that minimize radiation for $V = 0.93$.FIG. 30: Fraction of the total energy of initial configuration carried out by radiation for $v = 0.45$.

D. Non-symmetric configurations

The simplest non-symmetric configurations are given by oscillons that differ by their phases. In order to probe this class of scattering, we use initial conditions given by (III.12) taken at time $t = 0$. In Figs.31(a-d) we plot four cases of the time evolution for these processes. Interestingly, there are non-symmetric configurations for which no radiation is present. Figs.31(b) and 31(d) show two of these cases.

In order to have a clearer picture on the amount of input energy converted to radiation, we plot a map much like the ones presented in Figs. 24 and 30, except in this case we fix the values $V = 0.93$ and $v = 0$, and vary the parameters α_L and α_R (now independent of each other). This map is shown in Fig. 32.

The dependence $\alpha_L = \alpha_R$ corresponds with symmetric configurations of the initial conditions, and is marked in this figure as a black dashed line. It passes through two minima in radiation, as is expected according to the results from Sec. III C. Along this line, this map has a coincident set of values with the map in Fig. 24 along the line given by $V = 0.93$. Also, as mentioned in Sec. III C 3, for null speeds of the borders ($v = 0$), a shift of $\frac{1}{2}$ in the phase of a given oscillon will produce the same oscillon with a sign change in the value of its field and time derivative. For this reason, the relation $\alpha_R = \alpha_L \pm \frac{1}{2}$ corresponds to anti-symmetric initial field configurations. This relation is marked on the figure as the two dot-dashed white lines. In agreement with the results from Sec. III B, these lines lie on top of dark regions that correspond to no-radiation zones.

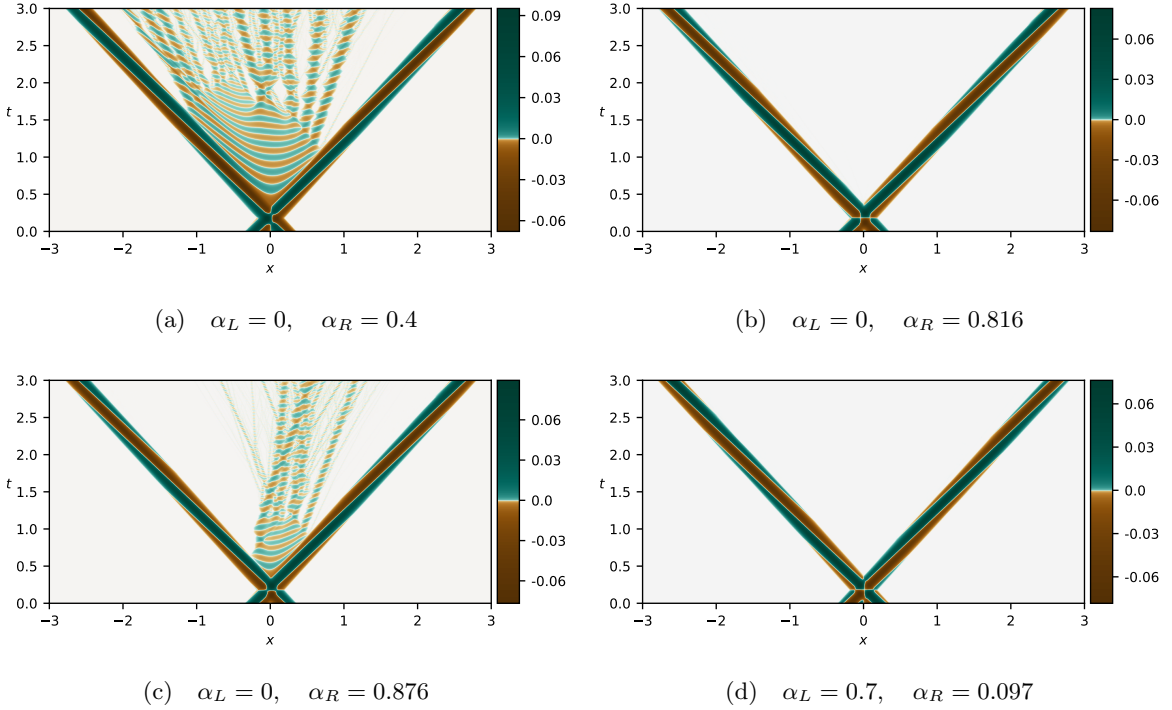


FIG. 31: The scattering process for initial configuration containing oscillons with speed $V = 0.93$, velocity of the border $v = 0$ and different phases α_1 and α_2 .

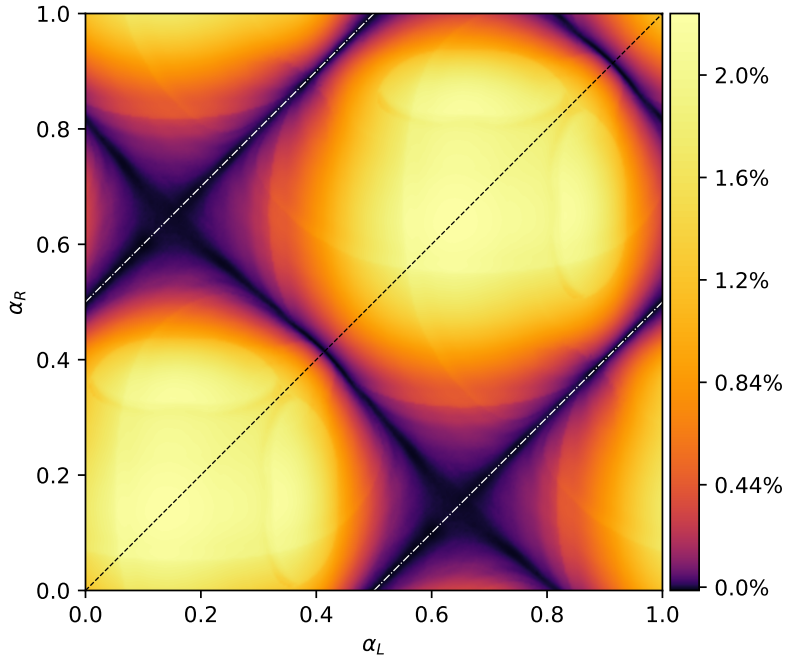


FIG. 32: Fraction of the total energy of initial configuration carried out by radiation in dependence on phases of oscillons α_L and α_R for $V = 0.93$. The black dashed line corresponds to the set of all symmetric such configurations and the white dot-dashed lines correspond to the set of all anti-symmetric such configurations.

This map can be seen as periodic both in α_L as well as in α_R (although the phase is originally defined as a value between 0 and 1, the field configuration is precisely the same for both these values), leaving it with a toroidal topology. In this view, the two black strips marked by the white dot-dashed lines form a belt around the torus and become a single continuous region.

We note, still, a second strip of no-radiation forming a 90 degree angle with these lines. One could expect the eventual vanishing of radiation in non-symmetric initial scattering configurations *e.g.* Figs. (31b) and (31d). Yet, the regularity of this region (it is a straight line) is quite remarkable and requires further inspection.

We plot a similar map with α_L fixed and vary α_R and V . This map can be seen in Fig. (33) and, along the line given by $V = 0.93$, its values coincide with those in Fig. (32) for $\alpha_L = 0$.

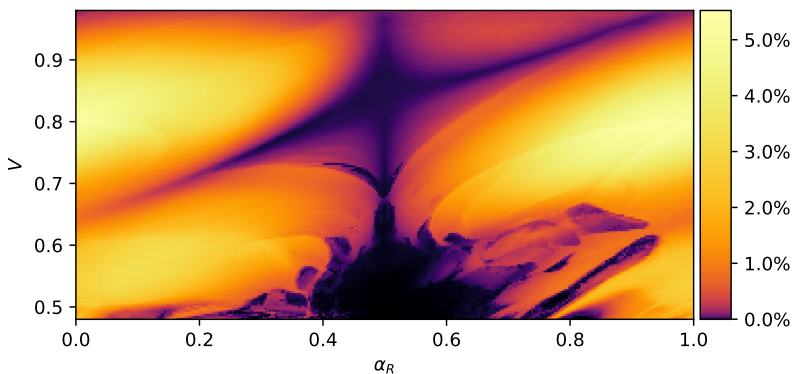


FIG. 33: Fraction of the total energy of initial configuration carried out by radiation in dependence on the input speed V and phase of right input oscillon α_R while holding fixed the right input oscillon's phase $\alpha_R = 0$.

The strip along $\alpha_R = \frac{1}{2}$ corresponds to anti-symmetric configurations and as a consequence it shows little or no radiation around it. Below the value $V \simeq 0.7$ there appears a large irregular region devoid of radiation. From the standpoint of numerical stability of our methods for the measure of radiation in regions of low V , as mentioned in Sec. III F, this region could well be a consequence of numerical artifacts. In a brief investigation of this hypothesis, though, we find this void to actually be an accurate description, and the region indeed represents a zone of no-radiation interactions for very low energy input (low boosts). So the value $V \simeq 0.7$ is crytical in the sense that, below it, an entire region in this particular set of values in the parameter space generates initial conditions to scattering that produces no radiation, and the region doesn't seem to have a very well defined shape.

One possible explanation for this void is that there is indeed generation of radiation in the scattering process but the radiation happens to be consumed by the outgoing oscillons, which in turn become more perturbed. This hypothesis can be checked by observing the energy of each outgoing oscillon independently on this region. In Figs. (34a,b) we plot the energy balance of each outgoing oscillon compared to its initial energy. This balance is calculated by

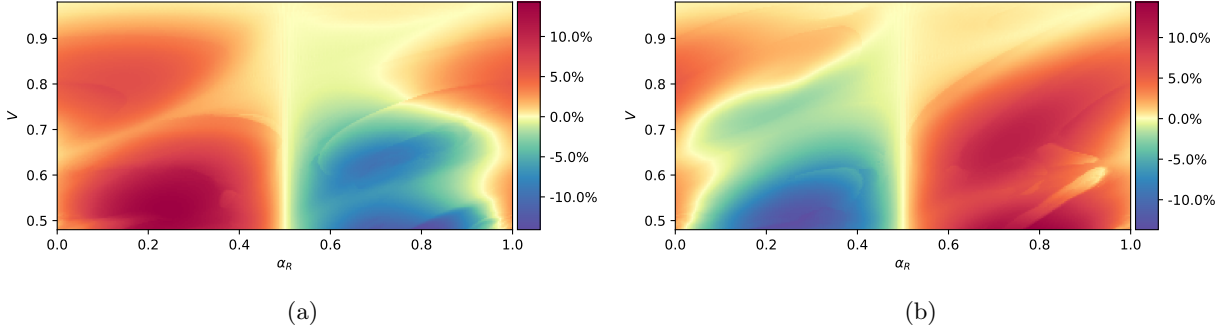


FIG. 34: Balance of energy after interaction (in percentage of incident energy) for each oscillon, where (a) is for the left outgoing oscillon and (b) for the right outgoing oscillon.

$$\Delta E_L = 1 - \frac{E_L}{E/2}$$

$$\Delta E_R = 1 - \frac{E_R}{E/2},$$

where E_L is the energy of the left outgoing oscillon (which entered by the right), E_R is the energy of the right outgoing oscillon and E the total input energy. Note that the map on Fig. 33 shows the value of amount of energy lost to radiation, given by

$$E_{rad} = 1 - \frac{E_L + E_R}{E}$$

$$= \frac{1}{2}(\Delta E_L + \Delta E_R),$$

so the total radiation is just the sum of energy balance of individual scattered oscillons.

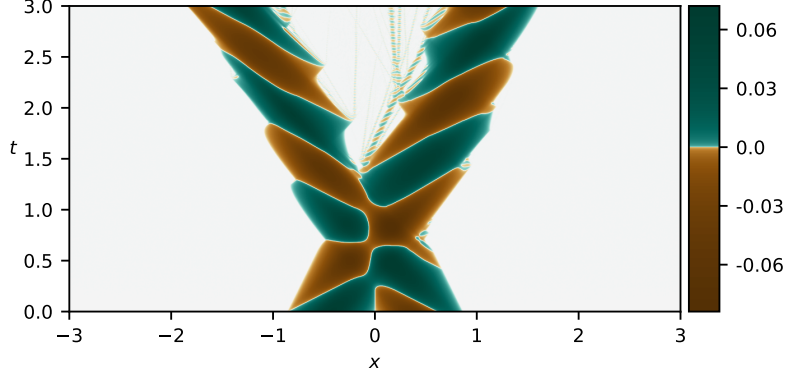


FIG. 35: Scattering process for $V = 0.5$ and $\alpha_2 = 0.642$, with parameters α_1, v_1, v_2 all set to zero.

In these figures (Figs. (34a,b)) we can see that each oscillon loses/gains a considerable amount of energy in the process. This amount is close to up to 15% of each oscillon's incident energy in some cases, yet the total radiation generated is no larger than about 5.5% of the total incident energy. In Fig. 35 we show the case for $V = 0.5$, $\alpha_1 = 0$, $\alpha_2 = 0.642$, $v_1 = 0 = v_2$, that corresponds to a configuration which produces no radiation (it is within the void region) and at the same time

has a relatively large energy transfer between the two interacting oscillons (in the energy balance maps these regions show a lot of energy change in both oscillons). Note how the left input oscillon (outgoing towards the right) is larger than the one outgoing to the left. Most such configurations seem to reproduce this behavior, and the channel through which this energy is transferred, in all cases, seems to be related to the scale of the outgoing oscillons.

E. Oscillons with accelerating border

Looking at figures Fig.17 and Fig.13 we note that the outgoing oscillons are significantly different from the generalized oscillon with uniformly moving borders. The principal difference is notable in the form of world-lines corresponding with borders of the oscillons which take the form of rather curves than zig-zag piecewise straight lines. Moreover, the curves are surprisingly regular in shape what suggest the outgoing objects are not just simple perturbations of the generalized oscillons. Recently in [27] further generalization of the signum-Gordon oscillons has been proposed. This generalization allows to obtain oscillons with borders that are arbitrary time-like curves. We shall present here a construction of oscillons with a curvilinear borders and show pictures of such oscillons after applying a Lorentz boost.

1. General properties

For an oscillon with period T the complete solution can be constructed from the restriction of the solution $\varphi(t, x)$ for the interval $0 \leq t \leq T/2$. Similarly to the oscillons already known, we can get periodic and localized solutions demanding the conditions

$$\varphi(0, x) = \varphi\left(\frac{T}{2}, x\right) = 0, \quad (\text{III.20})$$

$$\partial_t \varphi(0, x) = \begin{cases} 0 & \text{if } x < 0 \\ f(x) & \text{if } 0 \leq x \leq T \\ 0 & \text{if } x > T \end{cases} \quad (\text{III.21})$$

where $f(x)$ is a continuous function such that $f(x) \leq 0$ for all $0 \leq x \leq T$ and $f(0) = f(T) = 0$. As a consequence, we assume that the solution $\varphi(t, x)$ is negative for $0 \leq t \leq T/2$.

The oscillon solution is localized in the sense that it is nonzero only in the region between two time-like curves γ_L and γ_R – the borders of the oscillon. The right border is a displacement by T of the left curve, so that the size of the oscillon remains constant. For $t \in [0, T/2]$ the borders move to the right by Δ and, for $t \in [T/2, T]$, the borders move in the opposite direction – returning to the original position.

The conditions (III.20) and (III.21) are satisfied assuming the following ansatz for the non-zero

part of the solution:

$$\varphi(t, x) = \begin{cases} F(x+t) - F(x-t+T) + \frac{t^2}{2} - \frac{T^2}{8} & \text{if } -t < x < t \\ F(x+t) - F(x-t) + \frac{t^2}{2} & \text{if } t < x < T-t \\ F(x+t-T) - F(x-t) + \frac{t^2}{2} - \frac{T^2}{8} & \text{if } T-t < x < T+t \end{cases} \quad (\text{III.22})$$

where $F(x)$ satisfies:

$$F(T) = F(0) - \frac{T^2}{8}, \quad (\text{III.23})$$

$$\frac{dF(x)}{dx} = \frac{f(x)}{2}. \quad (\text{III.24})$$

We demand, likewise for less general oscillons, that the solution approaches zero smoothly at the left border γ_L *i.e.* for a partial solution (III.22) at $-t < x < t$ it holds

$$\partial_x \varphi(t, x)|_{\gamma_L} = 0 \quad (\text{III.25})$$

where points belonging to the curve γ_L have coordinates related by $x = x(t)$. Expressing condition (III.25) in light-cone coordinates

$$y_{\pm} = x \pm t \quad (\text{III.26})$$

we get

$$\left(1 + \frac{dy_+}{dy_-}\right) \left(1 - 2 \frac{dy_+}{dy_-}\right) \partial_+ \varphi(y_+, y_-)|_{\gamma_L} = 0 \quad (\text{III.27})$$

where we have used the fact that (y_+, y_-) are related and $\frac{dy_+}{dy_-} = -\frac{1}{2} \frac{dx}{dt}$. Since γ_L is a time-like curve then $|\frac{dy_+}{dy_-}| < \frac{1}{2}$ and so condition (III.27) is equivalent to $\partial_+ \varphi(y_+, y_-)|_{\gamma_L} = 0$. It results in $F'(y_+) = -\frac{1}{4}(y_+ - y_-)$ for first expression of (III.22). Taking into account expression (III.24) we finally get

$$f(y_+) = -\frac{1}{2}(y_+ - y_-) \quad (\text{III.28})$$

where $y_- = g(y_+)$ is a function of y_+ representing left border of the oscillon (world-line γ_L). Similarly, demanding that $\partial_x \varphi(t, x)|_{\gamma_R} = 0$ at the right border of the oscillon γ_R we get condition which if written in dependence on y_- takes the form $\partial_- \varphi(y_+, y_-)|_{\gamma_R} = 0$. Then from the last expression of (III.22) we get

$$f(y_-) = -\frac{1}{2}(y_+ - y_-). \quad (\text{III.29})$$

Here $y_+ = h(y_-)$ is a function of y_- representing right border of the oscillon (world-line γ_R). Note that for points on γ_L we have $0 \leq y_+ \leq T/2 + \Delta$ and for points on γ_R we have $T/2 + \Delta \leq y_- \leq T$. Thus, (III.28) determines $f(x)$ for $0 \leq x \leq T/2 + \Delta$ and (III.29) for $T/2 + \Delta \leq x \leq T$.

Using this formalism, all oscillon solutions limited by a pair of time-like curves identical to one another can be constructed by plugging the *a priori* given trajectories of the border in (III.28) and (III.29). The trajectories should have such a form that one can be able to describe them explicitly in the form $y_- = g(y_+)$ for γ_L and $y_+ = h(y_-)$ for γ_R . The only difficulty remaining is to integrate the resulting expressions to get $F(x)$ – and consequently $\varphi(t, x)$.

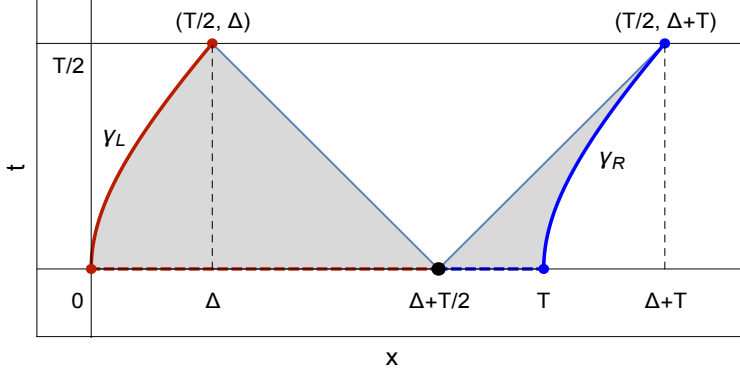


FIG. 36: Borders γ_L and γ_R of the oscillon and the supports $[0, \Delta + T/2]$ and $[\Delta + T/2, T]$ of $f(x)$.

2. Example

The first interesting example we can find is an oscillon with borders having a constant acceleration a in the instantaneous rest frame of the border. We shall use units in which $c = 1$. In the reference frame of the oscillon, in which the border has acceleration $\gamma^{-3}a$, the trajectory describing motion of such borders reads

$$x(t) = x_0 + \frac{1}{a} \left[\sqrt{1 + (at + \gamma_0 v_0)^2} - \gamma_0 \right] \quad (\text{III.30})$$

where v_0 is the velocity of the border at $t = 0$, $\gamma_0 = (1 - v_0^2)^{-1/2}$ and $x_0 = 0$ ($x_0 = T$) for γ_L (γ_R). Note that if the oscillon has no extra motion than its rest frame is just the laboratory reference frame. Using light-cone coordinates $y_{\pm} = x \pm t$ one can put the expression (III.30) in the form $y_- = g(y_+)$, where $x_0 = 0$, and $y_+ = h(y_-)$, where $x_0 = T$. Then plugging these expressions to (III.28) and (III.29) one gets an explicit expression for $f(x)$:

$$f(x) = \begin{cases} -\frac{x}{2} \left(1 + \frac{B}{x+A} \right) & \text{if } 0 \leq x \leq \frac{T}{2} + \Delta \\ \frac{x-T}{2} \left(1 + \frac{A}{x-T+B} \right) & \text{if } \frac{T}{2} + \Delta \leq x \leq T. \end{cases} \quad (\text{III.31})$$

where

$$A = \frac{\gamma_0(1 + v_0)}{a}, \quad (\text{III.32})$$

$$B = \frac{\gamma_0(1 - v_0)}{a}. \quad (\text{III.33})$$

Once we know $f(x)$, it is possible to integrate it and get partial solutions $\varphi_k(t, x)$ with $k \in \{C, L_1, L_2, L_3, R_1, R_2, R_3\}$, each one valid in a specific subset of the region between γ_L and γ_R .

Such solutions are given by:

$$\begin{aligned}\varphi_C(t, x; A, B) = & -\frac{AB}{4} + \frac{1}{4}(x + t + B - T)(x - t + A) + t\left(t - \frac{T}{2}\right) \\ & - \frac{AB}{4} \ln \left| \frac{1}{AB}(x + t + B - T)(x - t + A) \right|,\end{aligned}\quad (\text{III.34})$$

$$\varphi_{L_1}(t, x; A, B) = \frac{t}{2}(t - x - B) + \frac{AB}{4} \ln \left| \frac{x + t + A}{x - t + A} \right|, \quad (\text{III.35})$$

$$\begin{aligned}\varphi_{L_2}(t, x; A, B) = & \frac{AB}{4} - \frac{1}{4}(x + t + A)(x - t + B) \\ & + \frac{AB}{4} \ln \left| \frac{1}{AB}(x + t + A)(x - t + B) \right|,\end{aligned}\quad (\text{III.36})$$

$$\varphi_{L_3}(t, x; A, B) = \frac{1}{2}\left(t - \frac{T}{2}\right)(x + t + A) - \frac{AB}{4} \ln \left| \frac{x + t + B - T}{x - t + B} \right| \quad (\text{III.37})$$

where $AB = a^{-2}$. Similarly to the oscillons previously presented, we can relate the solutions $\varphi_{R_i}(t, x)$ with the solutions $\varphi_{L_i}(t, x)$ through the transformations:

$$x \rightarrow T - x, \quad (\text{III.38})$$

$$v_0 \rightarrow -v_0, \quad (\text{III.39})$$

$$a \rightarrow -a. \quad (\text{III.40})$$

Notice that the last two transformations are equivalent to the transformations:

$$A \rightarrow -B, \quad (\text{III.41})$$

$$B \rightarrow -A. \quad (\text{III.42})$$

Thus we have

$$\varphi_{R_i}(t, x; A, B) = \varphi_{L_i}(t, T - x; -B, -A). \quad (\text{III.43})$$

Once again we can write the full solution with the help of the step functions:

$$\begin{aligned}\Pi_C(t, x; a, v_0) = & \theta\left(x + t - \frac{T}{2} - \Delta(a, v_0)\right) \theta(x - t) \times \\ & \times \theta\left(-x + t + \frac{T}{2} + \Delta(a, v_0)\right) \theta(-x - t + T),\end{aligned}\quad (\text{III.44})$$

$$\Pi_{L_1}(t, x; a, v_0) = \theta(x - t) \theta\left(-x - t + \frac{T}{2} + \Delta(a, v_0)\right), \quad (\text{III.45})$$

$$\begin{aligned}\Pi_{L_2}(t, x; a, v_0) = & \theta\left(x - \frac{1}{a}\left(\sqrt{1 + (at + \gamma_0 v_0)^2} - \gamma_0\right)\right) \times \\ & \times \theta(-x + t) \theta\left(-x - t + \frac{T}{2} + \Delta(a, v_0)\right),\end{aligned}\quad (\text{III.46})$$

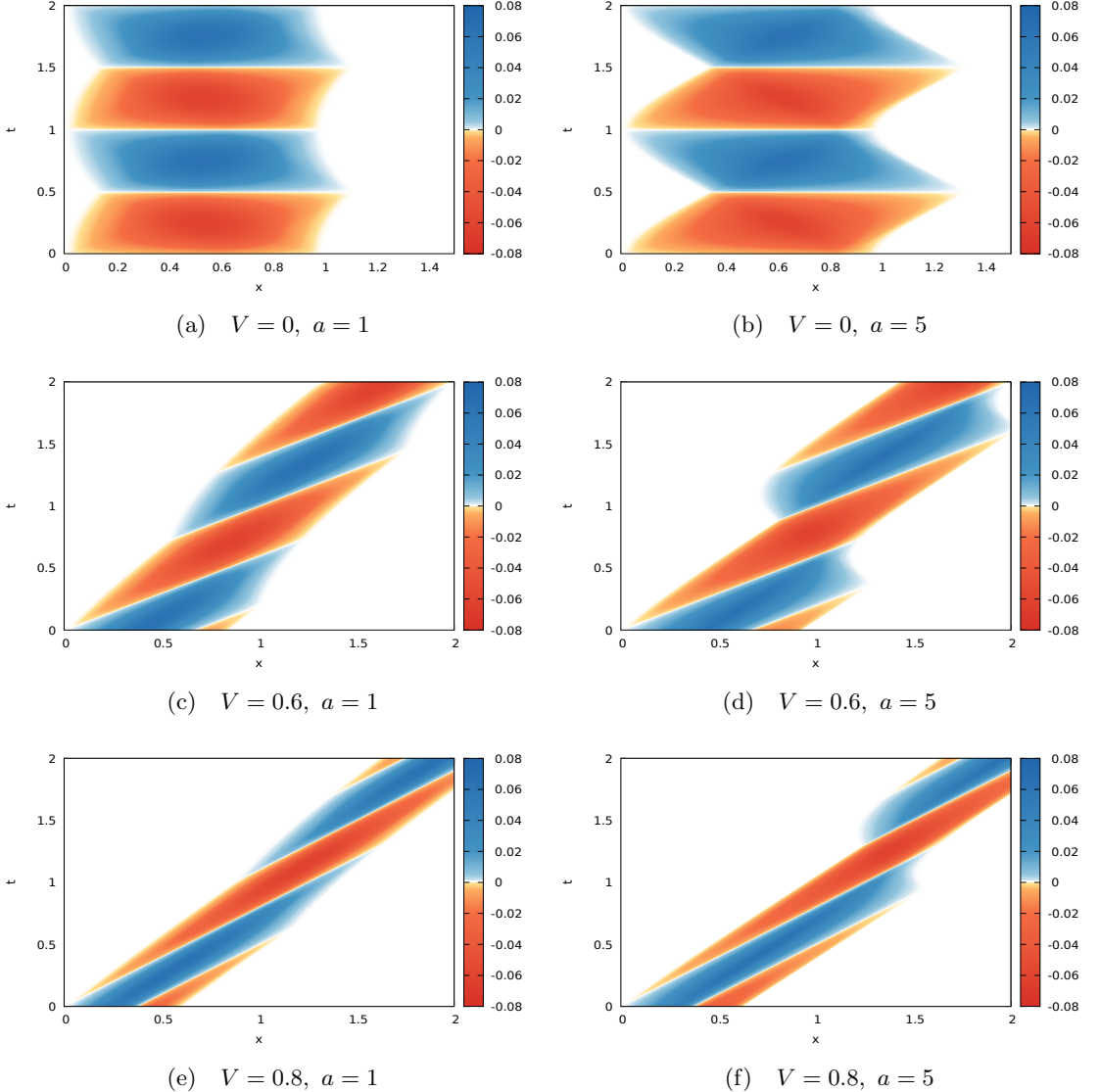


FIG. 37: Exact oscillon with uniformly accelerated border for different values of the boost velocity V and acceleration a .

$$\Pi_{L_3}(t, x; a, v_0) = \theta(-x + t)\theta\left(x + t - \frac{T}{2} - \Delta(a, v_0)\right), \quad (\text{III.47})$$

$$\Pi_{R_i}(t, x; a, v_0) = \Pi_{L_i}(t, T - x; -a, -v_0), \quad (\text{III.48})$$

where $\Delta = x(T/2) - x_0$ can be expressed as the function

$$\Delta(a, v_0) = \frac{1}{a} \left[\sqrt{1 + \left(a \frac{T}{2} + \gamma_0 v_0\right)^2} - \gamma_0 \right]. \quad (\text{III.49})$$

The periodicity of the solution can be taken into account by a generalized form of the functions

$\tau(z)$ and $\sigma(z)$ for an arbitrary period T :

$$\tau(z) = \frac{T}{\pi} \arcsin \left| \sin \left(\frac{\pi z}{T} \right) \right| \quad (\text{III.50})$$

$$\sigma(z) = \operatorname{sgn} \left(\sin \left(\frac{2\pi z}{T} \right) \right). \quad (\text{III.51})$$

Therefore, the complete solution has the form:

$$\varphi(t, x; a, v_0) = \sum_k \sigma(t) \Pi_k(\tau(t), x; a, v_0) \varphi_k(\tau(t), x; A(a, v_0), B(a, v_0)) \quad (\text{III.52})$$

where $A(a, v_0)$ and $B(a, v_0)$ are given by (III.32) and (III.33).

F. Fractal nature of the radiation

Looking at results of our numerical simulations we see that radiation of the signum-Gordon model is dominated by oscillating structures that looks like traveling oscillons. In fact, a production of small-size oscillons during the evolution of perturbed oscillons has been conjectured in the remark part of Ref. [25]. This conjecture was motivated by the dilation symmetry of the signum-Gordon equation (I.2). Let $\lambda > 0$ be certain real number and $\phi_{(1)}(t, x)$ be a solution of the signum-Gordon equation. The dilation symmetry means that

$$\phi_{(\lambda)}(t, x) := \lambda^2 \phi_{(1)}\left(\frac{t}{\lambda}, \frac{x}{\lambda}\right) \quad (\text{III.53})$$

is also a solution of (I.2). Looking at energy of solutions we see that it scales according to

$$E[\phi_{(\lambda)}] = \lambda^3 E[\phi_{(1)}] \quad (\text{III.54})$$

where

$$E[\phi_{(1)}] := \int_{-\infty}^{\infty} dx \left[\frac{1}{2} (\partial_t \phi_{(1)})^2 + \frac{1}{2} (\partial_x \phi_{(1)})^2 + |\phi_{(1)}| \right]. \quad (\text{III.55})$$

In particular, the exact oscillon on a segment $x \in [0, 1]$ has energy $E[\phi_{(1)}] = \frac{1}{24}$. Note that generalized oscillons with uniformly or non-uniformly moving borders have exactly the same energy. The dilation symmetry allows for the existence of exact compact oscillons with arbitrarily small support. A set of such oscillons with non-overlapping supports constitute a multi-oscillon solutions. Moreover, one can Lorentz boost each such oscillon independently on other oscillons and they will remain exact solutions until they collide with other oscillons.

Although we do not expect that oscillations seen in our numerical simulations are exact oscillons we can call them *quase-oscillons* because they are amazingly stable and regular. Less regular structures “decay” emitting smaller and more regular oscillating objects. Thus the emission of quase-oscillons seems to be a physical mechanism allowing that strongly perturbed oscillons get rid of a surplus of their energy and became more regular. Such smaller quase-oscillons can furthermore emit other small oscillons. Since they have some linear momentum the collisions with other quase-oscillons are unavoidable. These collisions are responsible for production of other quase-oscillons.

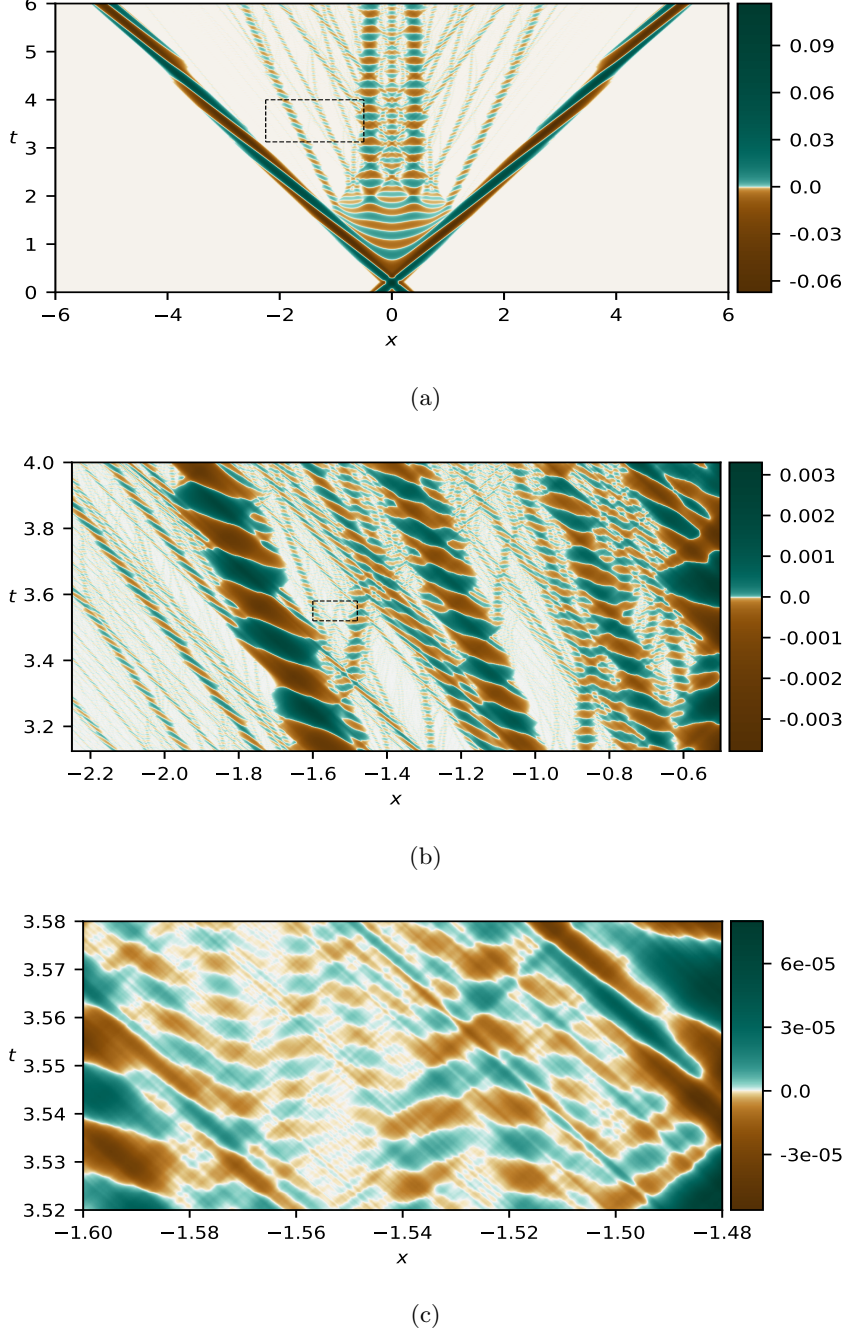


FIG. 38: Scattering process of two oscillons: (b) blow-up of rectangular region on (a); (c) blow-up of rectangular region in (b).

Note that relation (III.53) can be applied to a solution representing a whole scattering process. Certainly, there is no qualitative difference between scattering process involving two oscillons with $\lambda = 1$ and a scattering of smaller oscillons with $\lambda \ll 1$. The repetition of some structures involving oscillons in all length scales on the spacetime diagram suggests a fractal nature of a radiation.

In order to check our hypothesis we perform high resolution simulations of the scattering process and then look at the spacetime diagram representing the result. In Fig.38(a) we plot the two leading

outcomming oscillons and the radiation in the central region between these oscillons. Looking in more detail at the region inside the rectangle we see in Fig.38(b) that there exist huge number of smaller oscillons invisible in the previous picture. Choosing another rectangular region we see in Fig.38(c) that it contains a plenty of oscillating structures. This result supports our idea about fractal nature of the radiation of the signum-Gordon model.

Finally we would like to comment about difficulties associated with numerical integration of the signum-Gordon equation. The main difficulty has origin in the fact that the radiation contains perturbed oscillons with arbitrarily small size. Certainly, oscillons smaller than the size of numerical domain cannot be seen in the simulation. An obvious solution is increasing the number of points in the grid. We have run many simulations changing the number of points and comparing the results. This test has shown that very small oscillons are sensible on the number of points. In some cases changing the number of points by factor two resulted in appearance or even disappearance of some tiny structures whereas bigger structures were stable under this procedure. The similar problem was spotted in simulations of a special type of self-similar solution with infinite number of zeros on a finite segment. In that case the numerical solution and the analytical one diverged after short time. On the other hand, our numerical simulations of the exact oscillons did not lead to visible instability within intervals of time corresponding with many oscillon periods. Also simulations of exact shock waves were very consistent with analytical solutions. Thus in the regions dominated by radiation (or a special self-similar solution) the solutions of the model are very sensible on initial conditions. In this sense the signum-Gordon model could share some properties with chaotic systems. This property is a principal difficulty in generating of high resolution fractals.

IV. CONCLUSIONS

In this paper we have reported on results of scattering of compact oscillons in the signum-Gordon model in one spatial dimension. We have looked at two qualitatively distinct initial configurations – symmetric and anti-symmetric one. In both cases the initial configuration consist on exact compact solutions. Due to compactness of oscillons there is no problem with their overlapping at $t = 0$. In fact we take oscillons which supports touch each other but do not overlap at $t = 0$. A time dependence of the shape of oscillons is responsible for existence of additional scattering parameter which we call phase of the oscillon. This phase is a relevant quantity which the scattering process depends on.

Looking at results of scattering of oscillons we see that there is significant qualitative difference between symmetric and anti-symmetric initial configurations. The emission of radiation for anti-symmetric configurations is restricted to situations where outgoing oscillons have irregular borders. Such irregular borders act as sources of radiation which have the form of smaller oscillons send out from the borders. The central region of the Minkowski diagrams just after emergence of outgoing oscillons is free of radiation. On the other hand, symmetric configurations produce much more radiation than the anti-symmetric ones. In this case the radiation is emitted mainly in the central part of the Minkowski diagram where forms a structure similar to exact shock wave solution of the signum-Gordon model. This wave apparently is not stable and eventually decays in a cascade

of oscillons. We have spotted that there are special values of phases of colliding oscillons where there is almost no radiation. We suspect that this fact is associated with absence of the shockwave-like structure between outgoing oscillons. The relation between collapse (decay) of shockwave-like solution and appearance of cascade of oscillons is a very interesting subject, however, it requires thorough analysis. Such an analysis is out of the main scope of this paper. We shall report on this subject in near future.

Comparing incoming oscillons with outgoing ones we have spotted that in generality the later ones belong to a wider class of oscillons. This class is characterized by non-uniform motion of the border of the ooscillon in its own rest frame. In our numerical study many of outgoing oscillons have border given by a segment of the curve world-line whereas of for incoming oscillons this borders are segments of straight lines. Thus the collision transforms compact oscillons of a given class into more general compact oscillons.

Finally, we have looked at the radiation of the signum-Gordon model as on the self-similar structure. Since the model has the scaling symmetry one can show that exact compact oscillon can have arbitrarily small support and energy. Numerics shows that small oscillons are emitted from perturber oscillons. Since in generality they are also perturbed the process of emission repeats (in principle infinitely many times). The mechanism of emission of oscillons from perturbed objects and the fact that oscillons exists in arbitrarily small scales gives rise to appearance of dynamical fractals i.e. fractal structures on the spacetime diagram. We called them world-trees as they consists on world-sheets of oscillons which contains infinite number of ramifications.

Acknowledgements

The authors are grateful to H. Arodz, A. Wereszczynski and Z. Świerczyński for discussion and comments. PK wants to thank Faculty of Physics, Astronomy and Applied of Computer Science of the Jagiellonian University for financial support and hospitality during the symposium *The nonperturbative world* in honor of Prof. Henryk Arodz on the occasion of his 70th birthday where some preliminary result of this paper were reported. FMH is supported by CNPq Scholarship. This study was financed in part by the Coordenação de Aperfeiçoamento de Pessoal de Nível Superior a Brasil (CAPES) Finance Code 001.

- [1] I. L. Bogolyubsky and V. G. Makhankov, Pis'ma v Zhurnal Èksperimental'noi i Teoreticheskoi Fiziki, 24 (1976) 15.
- [2] M. Gleiser, Pseudostable bubbles, Phys. Rev. D 49 (1994) 2978
- [3] M. Gleiser, Oscillons in scalar field theories: applications in higher dimensions and inflation, Int. J. Mod. Phys. D 16 (2007) 219
- [4] M. Gleiser and M. Krackow, Resonant Configurations in Scalar Field Theories: Can (Some) Oscillons Live Forever?, [hep-th 1906.04070]
- [5] Y. M. Shnir, Topological and Non-Topological Solitons in Scalar Field Theories, Cambridge University Press (2018)

- [6] P. Salmi and M. Hindmarsh, Radiation and relaxation of oscillons, *Phys. Rev. D* 85 (2012) 085033
- [7] G. Fodor, P. Forgacs, P. Grandclement and I. Racz, Oscillons and quasi-breathers in the ϕ^4 Klein-Gordon model, *Phys. Rev. D* 74 (2006) 124003
- [8] G. Fodor, P. Forgacs, Z. Horvath, and A. Lukács, Small amplitude quasibreathers and oscillons, *Phys. Rev. D* 78 (2008) 025003
- [9] T. Romańczukiewicz and Y. Shnir, Oscillon resonances and creation of kinks in particle collisions, *Phys. Rev. Lett.* 105 (2010) 081601
- [10] T. Romańczukiewicz and Y. Shnir, Oscillons in the presence of external potential, *J. High Energ. Phys.* 01 (2018) 101
- [11] R. A. C. Correa, W. de Paula, T. Frederico, O. Oliveira, F. E. M. Silveira, Oscillons in ϕ^6 -theories: Possible occurrence in MHD, [hep-th 1806.04412]
- [12] R. A. C. Correa, A. de Souza Dutra, T. Frederico, Boris A. Malomed, O. de Oliveira, N. Sawado, Creating Oscillons and Oscillating Kinks in Two Scalar Field Theories, [hep-th 1907.07145]
- [13] J. Sakstein and M. Trodden, Oscillons in higher-derivative effective field theories, *Phys. Rev. D* 98 (2018) 123512
- [14] C. Adam, T. Romańczukiewicz, and A. Wereszczynski, The ϕ^4 model with the BPS preserving defect, *J. High Energ. Phys.* 03 (2019) 131
- [15] T. Romańczukiewicz, Y. Shnir, Some Recent Developments on Kink Collisions and Related Topics, Kevrekidis P., Cuevas-Maraver J. (eds) A Dynamical Perspective on the ϕ^4 Model.
- [16] D. Bazeia, E. Belendryasova, and V. A. Gani, Scattering of kinks in a non-polynomial model, IOP Conf. Series: Journal of Physics: Conf. Series 934 (2017) 012032
- [17] D. Bazeia, E. Belendryasova, V.A. Gani, Scattering of kinks in a non-polynomial model. *J. Phys. Conf. Ser.* 934 (2017) 012032
- [18] A. Alonso Izquierdo, Kink dynamics in the MSTB model, *Phys. Scr.* 94 (2019) 085302
- [19] M. J. Ablowitz, D. J. Kaup, A. C. Newell, and H. Segur, Method for Solving the Sine-Gordon Equation, *Phys. Rev. Lett.* 30 (1973) 1262
- [20] Mark J. Ablowitz, David J. Kaup, Alan C. Newell, and Harvey Segur, Nonlinear-Evolution Equations of Physical Significance *Phys. Rev. Lett.* 31 (1973) 125
- [21] L.A. Ferreira, W.J. Zakrzewski, A simple formula for the conserved charges of soliton theories, *J. High Energ. Phys.* 09 (2007) 015
- [22] D.I. Olive, N. Turok. J.W.R.Underwood, Affine Toda solitons and vertex operators, *Nucl. Phys. B* 409 (1993) 509
- [23] M. Tajiri and Y. Watanabe, Breather solutions to the focusing nonlinear Schrödinger equation, *Phys. Rev. E* 57 (1998) 3510
- [24] D.J. Kedziora, A. Ankiewicz, and N. Akhmediev, Second-order nonlinear Schrödinger equation breather solutions in the degenerate and rogue wave limits, *Phys. Rev. E* 85 (2012) 066601
- [25] H. Arodź, P. Klimas, T. Tyranowski, Compact oscillons in the signum-Gordon model, *Phys. Rev. D* 77, 047701 (2008)
- [26] H. Arodź, Z. Swierczyński, Swaying oscillons in the signum-Gordon model, *Phys. Rev. D* 84 (2011) 067701
- [27] Z. Świerczyński (2017), On the oscillons in the signum-Gordon model, *Journal of Nonlinear Mathematical Physics*, 24:1, 20-28
- [28] H. Arodź, P. Klimas, T. Tyranowski, Field-Theoretic Models with V-Shaped Potentials, *Acta Phys. Pol. B* 36 (2005) 3861
- [29] H. Arodź, Topological Compactons, *Acta Phys. Pol. B* 33 (2002) 1241
- [30] D. Bazeia, L. Losano, M.A. Marques, R. Menezes, R. da Rocha, Compact Q-balls, *Physics Letters B*

758 (2016) 146

[31] D. Bazeia, M. A. Marques and R. Menezes, Compact lumps, *EPL* 111 (2015) 61002

[32] D. Bazeia, L. Losano, M.A. Marques, R. Menezes, Compact structures in standard field theory, *EPL* 107 (2014) 61001

[33] D. Bazeia, L. Losano, M.A. Marques, R. Menezes, Compact Chern Simons vortices, *Physics Letters B* 772 (2017) 253

[34] D. Bazeia, E. da Hora, and D. Rubiera-Garcia, Compact vortexlike solutions in a generalized Born-Infeld model, *Phys. Rev. D* 84 (2011) 125005

[35] H. Arodź, P. Klimas, T. Tyranowski, Scaling, self-similar solutions and shock waves for V-shaped field potentials, *Phys. Rev. E* 73 (2006) 046609

[36] C. Adam, D. Foster, S. Krusch, and A. Wereszczynski, BPS sectors of the Skyrme model and their non-BPS extensions, *Phys. Rev. D* 97 (2018) 036002

[37] C. Adam, P. Klimas, J. Sanchez-Guillen, and A. Wereszczynski, Compact baby Skyrmions, *Phys. Rev. D* 80 (2009) 105013

[38] P. Klimas, J. S. Streibel, A. Wereszczynski, W. J. Zakrzewski, Oscillons in a perturbed signum-Gordon model, *J. High Energ. Phys.* 04 (2018) 102

[39] P. Klimas and L.R. Livramento, Compact Q-balls and Q-shells in CP^N -type models, *Phys. Rev. D* 96 (2017) 016001

[40] C. Adam, J. Sanchez-Guillen, and A. Wereszczynski, A Skyrme-type proposal for baryonic matter, *Phys. Lett. B* 691 (2010) 105